


Review Article

Open Access



Biomedical sensing applications of soft, wearable microfluidic systems

Muhammad Sohail Ibrahim^{1,2}, Abdul Naman², Myeong-Seok Lee², Sejin Park², Dongho Lee², Yunsang Kwak², Minseok Kim^{1,2,3,*} 

¹On-Sensor AI Semiconductor Center, Kumoh National Institute of Technology, Gumi-si 39177, Republic of Korea.

²Department of Mechanical Engineering, Kumoh National Institute of Technology, Gumi-si 39177, Republic of Korea.

³Department of Aeronautics, Mechanical and Electronic Convergence Engineering, Kumoh National Institute of Technology, Gumi-si 39177, Republic of Korea.

*Correspondence to: Prof. Minseok Kim, Department of Mechanical Engineering, Kumoh National Institute of Technology, Gumi-si 39177, Republic of Korea. E-mail: mkim@kumoh.ac.kr

How to cite this article: Ibrahim, M. S.; Naman, A.; Lee, M. S.; Park, S.; Lee, D.; Kwak, Y.; Kim, M. Biomedical sensing applications of soft, wearable microfluidic systems. *Soft Sci.* 2025, 5, 49. <https://dx.doi.org/10.20517/ss.2025.45>

Received: 30 Jun 2025 **First Decision:** 25 Jul 2025 **Revised:** 3 Sep 2025 **Accepted:** 9 Sep 2025 **Published:** 10 Oct 2025

Academic Editors: YongAn Huang, Nae-Eung Lee, Nan Xiang **Copy Editor:** Pei-Yun Wang **Production Editor:** Pei-Yun Wang

Abstract

Soft microfluidic sensing platforms have emerged as a transformative technology for real-time, noninvasive, and continuous health monitoring. This paper reviews recent advancements in soft microfluidic systems, focusing on the biomedical sensing platforms such as colorimetric, electrochemical, optical, etc., sensing modalities. Additionally, the integration of multimodal sensing approaches is discussed as a strategy to enhance sensitivity, specificity, and robustness under dynamic physiological conditions. Key material and fabrication strategies enabling flexibility, stretchability, and biocompatibility are highlighted, along with their interfacing challenges in wearable formats. The review also explores the role of artificial intelligence in sensor design, data processing, and predictive diagnostics. By identifying current limitations and emerging trends, this work provides future directions toward developing next-generation soft microfluidic systems for personalized, decentralized healthcare.

Keywords: Soft microfluidics, wearable devices, sweat sensing, biosensors

INTRODUCTION

Soft, flexible, on-skin wearable devices and biosensors have gained significant attention in recent years owing to their ability to continuously sense and monitor various key biomarkers for biosensing and health



© The Author(s) 2025. **Open Access** This article is licensed under a Creative Commons Attribution 4.0 International License (<https://creativecommons.org/licenses/by/4.0/>), which permits unrestricted use, sharing, adaptation, distribution and reproduction in any medium or format, for any purpose, even commercially, as long as you give appropriate credit to the original author(s) and the source, provide a link to the Creative Commons license, and indicate if changes were made.



monitoring. Such on-skin, noninvasive devices can ensure improved personalized health monitoring while reducing medical costs, hospital visits, and associated hospitalization. Recent developments in wearable electronic devices enable accurate measurement of vital signals such as heart rate, temperature, and blood pressure; however, these biophysical signals lack direct insights into the dynamic metabolic and biochemical processes in the body. In this context, biofluids (such as sweat and tears), which are easy to sample, can potentially provide real-time and continuous physiological insights by examining the biomolecular state of the body.

Human biofluids contain rich biological information and serve as critical sources of biomarkers for monitoring health and physiological conditions. Among the various biofluids in human body, blood serves as the clinical gold standard for monitoring health and physiological conditions^[1]. Conventional handheld sensing platforms, such as blood analyzers, glucometers, *etc.*, rely heavily on invasive methods for sampling blood, thereby causing pain and risk to patients, significantly impeding the continuous measurement, monitoring, and analysis of the associated physiological signals. Current continuous monitoring systems rely on interstitial fluid; however, such interstitial fluid-based systems are categorized as minimally invasive, relying on small probes or microneedles to be implanted under the human skin^[2]. On the other hand, sweat is particularly well-suited for the noninvasive and continuous monitoring of various biomarkers. Densely distributed eccrine sweat glands become active during physical exertion and exercise, dispensing fluids that are rich in analytes such as metabolites, hormones, and electrolytes^[3]. Such biomolecules can potentially diffuse from blood or interstitial fluid into the sweat, thereby enabling continuous and real-time analysis and monitoring of the physiological condition of the individual under observation^[4]. Moreover, the concentration of several analytes is higher in sweat compared to other biofluids such as saliva, and can frequently correlate with the analyte levels in blood^[5]. However, significant challenges still persist, including lower sweat production rates, potential contamination from the skin and environment, *etc.*^[6].

Microfluidics is a multidisciplinary domain that deals with the precise manipulation and regulation of small volumes of fluids in geometrically designed microchannels. Microfluidic systems entail several practical applications such as particle manipulation, particle and cell sorting, gradient generation, *etc.*, and are widely used in the domains of cell culture, disease diagnosis, drug delivery, biochemistry, *etc.* These systems, often termed as lab-on-a-chip, offer promising integration opportunities with wearable sensors rendering sample-to-answer solutions. Soft and wearable microfluidic systems can enable noninvasive and continuous monitoring of physiological states and biomarkers in human body. Typical wearable microfluidic systems consist of an adhesive layer, polydimethylsiloxane (PDMS) substrate, microfluidic channels, biosensor layer, and a top PDMS layer. [Figure 1](#) presents a comprehensive overview of current designs and configurations of soft microfluidic systems used in wearable biosensing. The central schematic, presented in [Figure 1A](#), depicts a sweat-interfacing device composed of a biosensor, microfluidic channel, PDMS substrate, and adhesive layer, placed directly on skin over the sweat glands to enable continuous biomarker collection. Additional illustration, presented in [Figure 1B](#), shows the integration of various biosensing platforms such as colorimetric assays and other biosensing elements within PDMS-based microfluidic structures, enabling both quantitative and qualitative detection. The application of wearable devices across different anatomical sites [[Figure 1C](#)], such as the chest, hand, wrist, and eye, is illustrated to emphasize their flexibility and adaptability. Furthermore, the figure includes examples of biosensing using alternative biofluids, such as tears (via smart contact lenses) highlighting the expanding landscape of soft microfluidics beyond sweat-based monitoring. Together, these illustrations underscore the versatility and potential of soft microfluidic platforms for real-time, noninvasive health and exercise monitoring.

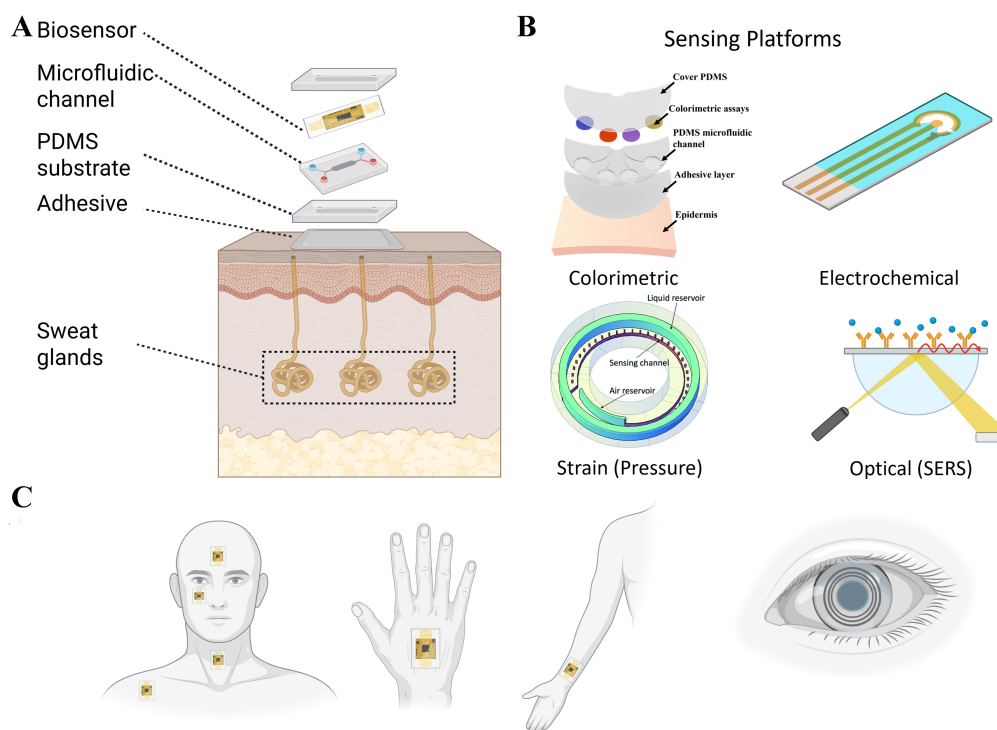


Figure 1. Overview of soft microfluidic systems for noninvasive biosensing applications. (A) Illustration of wearable platforms for sweat-based sensing; (B) integration strategies with colorimetric, electrochemical, optical, etc., sensing platforms; and (C) Common anatomical placement sites. Created with [BioRender.com](https://www.biorender.com).

During the past few years, several review contributions addressing the soft and wearable microfluidic platforms have been made. Gao *et al.* conducted a review discussing the role of flexible and wearable electrochemical sensors in the domain of sweat sensing and analysis^[7]. The study in^[8] presented a review focused on enzyme-based wearable biosensors detailing the convergence of engineering materials and integrating enzymes with electrodes to achieve effective biosensing in wearable platforms. The study in^[9] reviewed the microfluidics technology and fabrication techniques in handling biofluids in on-skin wearable devices. Sheffield *et al.* presented a review on the strategies and future research directions of wearable biosensors for the analysis and measurement of stress biomarkers targeting neuropsychiatric applications^[10]. However, the current review efforts either focus solely on a specific sensing domain or healthcare application. This study presents a review of the various sensing modalities used in soft wearable microfluidics for various applications such as healthcare, on-demand sweat analysis, exercise monitoring, disease diagnosis, *etc.* The sensing platforms include electrochemical, colorimetric, optical, among other innovative paradigms. Various sensing modalities and multiplex sensing platforms are also discussed. Avenues of possible future research and the integration of signal processing techniques are also discussed.

SOFT MICROFLUIDIC BIOSENSING PLATFORMS

Several fabrication materials have been used in the design of soft, wearable microfluidics such as PDMS, polymethylmethacrylate (PMMA), pressure sensing adhesive (PSA), hydrogels, smart textiles, *etc.*^[11,12]. Such wearable platforms are fabricated using various techniques such as soft lithography, laser cutting, 3D printing, *etc.*^[13,14]. These fabrication technologies enable the sophisticated creation of microchannels with various geometries, thereby supporting the integration of various functionalities and sensing platforms in a single wearable microfluidic device.

This section provides a review of the biosensing and transducing platforms commonly used in the soft and wearable microfluidic devices for noninvasive, continuous, and real-time health monitoring. The subsequent subsections provide comprehensive reviews of electrochemical, colorimetric, optical, multimodal, *etc.*, sensing platforms in wearable microfluidics.

Electrochemical sensing

Wearable electrochemical microfluidic systems mainly consist of three key components; the microfluidic device, electrochemical biosensor, and the associated electronic circuitry to process and transmit the data acquired by the sensors. Microfluidic electrochemical detection entails the use of an analyte solution containing the target biomarkers to be quantified. The quality of the microfluidic-based detection can be evaluated by measures such as sensitivity, limit of detection (LOD), and selectivity towards the target biomarker. Among the various biosensing platforms used in soft microfluidic devices, electrochemical sensing platforms are considered among the most widely used due to their high sensitivity and the signal processing ability offered by the associated electronics.

A recent study, presented in^[15], demonstrated a fully integrated wireless wearable patch for noninvasive, reagent-free monitoring of oestradiol in sweat using an aptamer-based electrochemical sensor. The system combines gold nanoparticles (AuNPs)–MXene electrodes with a target-induced strand displacement mechanism, enabling selective and sensitive detection of oestradiol in the picomolar range. The patch includes microfluidics carbachol-loaded iontophoretic stimulators, and flexible electronics for autonomous sweat induction, sampling, and signal transmission. The sensor showed high selectivity, strong correlation ($r = 0.921$) with enzyme-linked immunosorbent assay (ELISA), and regeneration capability, offering a promising platform for female hormone monitoring and personalized health tracking. The study in^[16] presented a flexible wearable immunosensor integrating $\text{Ti}_3\text{C}_2\text{T}_x$ MXene with laser-burned graphene on PDMS for electrochemical detection of cortisol in sweat. The microfluidic patch demonstrated high sensitivity with a LOD of 88 pM, offering a promising platform for noninvasive point-of-care stress monitoring. Similarly, the work in^[17] introduced a sustainable paper-based microfluidic immunosensor for reagent-free, wireless cortisol detection in sweat. Using a competitive magnetic bead-based assay and wax-printed capillary-driven channels, the device enables specific and flexible monitoring, validated during on-body cycling tests with near field communication (NFC)-based readout integration. A fully integrated, flexible organic electrochemical transistors with gold gate electrodes functionalized with monoclonal anticortisol antibodies for rapid, label-free cortisol detection in sweat is presented in^[18]. The electrochemical sensor achieved high sensitivity (50 $\mu\text{A}/\text{dec}$) across a 1–1,000 nM range with a 100 pM LOD, enabled by optimized poly(3,4-ethylenedioxythiophene) doped with poly(styrenesulfonate) (PEDOT:PSS) channel designs and gate capacitance modulation. Real-time detection is completed within five minutes, and results in sweat samples show strong agreement with liquid chromatography-tandem mass spectrometry analysis. The wearable format enables direct skin application for on-body, point-of-care stress monitoring. Other wearable microfluidic stress biomarker detection and monitoring solutions include; molecularly imprinted electrochemical sensor with a nanofiber-based microfluidic device for *in-situ* monitoring of cortisol^[19] and paper-based microfluidic device for cortisol detection^[20], wearable microfluidic patch aided with pseudoknot aptamer for real-time cortisol monitoring^[21], wearable sweat sensing patch equipped with a ternary composite electrode for continuous monitoring and analysis of stress biomarkers^[22], molecularly imprinted polymer (MIP)-radio-frequency wearable microfluidic system integrated with near-field communication for sweat cortisol monitoring^[23], wearable microfluidic electrochemical sensor with modified electrodes for noninvasive monitoring of oxidative stress (OS) biomarkers in human sweat^[24], wearable microfluidic sensing device, integrated with prestored reagents, for cortisol detection in sweat using aptamer as the recognition element^[25], soft microfluidic system equipped with organic electrolyte gated field-effect transistor aptasensor for cortisol testing in saliva^[26].

Soft microfluidic devices with electrochemical sensing have also been used in the detection, monitoring, and analysis of several biomarkers such as uric acid (UA), lactate, glucose, pH, and various ions such as sodium (Na^+), potassium (K^+), *etc.* The study in^[27] presented a multilayered, skin-interfaced microfluidic patch, as presented in Figure 2A, capable of continuous, noninvasive monitoring of sweat rate and biochemical composition during routine and physical activities. The patch incorporates, as depicted in Figure 2B, a hydrophilic filler composed of a patterned SU-8 mold, polyvinyl alcohol (PVA) film, and hydrogel within a collection well to reduce sweat secretion pressure and enhance sample acquisition. Sensing electrodes fabricated on a thin poly (ethylene terephthalate) (PET) substrate enable real-time analysis of sweat analytes, including pH and chloride ions. The patch was applied to different body locations, as presented in Figure 2C, including the wrist and fingertip, and used to monitor subjects during sedentary behavior and low-intensity activities such as sleeping, sitting, reading, and eating [Figure 2D]. Results, depicted in Figure 2E-G, demonstrate dynamic correlations between sweat secretion rate, heart rate, pH and chloride concentrations, without the need for externally stimulated sweating for the wearable sensor planted on the fingertip and wrist. This work underscores the feasibility of long-term, unobtrusive monitoring of physiological responses using soft microfluidic platforms in real-world, exercise-inclusive settings. The study in^[28] introduced a fully integrated, screen-printed epidermal microfluidic biosensing platform for real-time, multiplexed monitoring of sweat biomarkers during exercise. The system utilizes a cleanroom-free fabrication process that incorporates screen-printed carbon molds and flexible, low-cost materials to develop soft microfluidic channels and multiarray electrodes. The channels are chemically functionalized to enhance hydrophilicity and sweat transport, enabling rapid sample collection and delivery (within 40 s) to embedded sensing compartments. The wearable device supports simultaneous electrochemical sensing of lactate via amperometry and Na^+ , K^+ , and pH via potentiometry, using a miniature circuit board designed to eliminate signal interference and allow wireless data transmission. The lactate sensor employs a multilayer configuration combining carboxylic acid-functionalized single-walled carbon nanotube, Prussian Blue nanoparticles (NPs), and lactate oxidase for enhanced sensitivity and selectivity. Solid-state ion-selective electrodes and camphor sulphonic acid (CSA)-doped polyaniline-based pH sensors demonstrated high stability, reversibility, and minimal carryover. Human trials during stationary biking validated the capability of the system for real-time biomarker monitoring without external sweat stimulation. Regional variations in sweat composition at different skin locations (underarm and upper back) were analyzed. Overall, the platform offers a scalable, cost-effective solution for noninvasive biochemical monitoring, with strong potential for personalized health, athletic performance tracking, and point-of-care diagnostics.

A novel lactate biosensor integrated into a wearable microfluidic patch for real-time sweat monitoring during exercise and iontophoresis is presented in^[29]. The sensor employs a diffusion-limiting outer membrane that restricts lactate flux to the enzyme core, enabling an extended linear detection range (1-50 mM) and minimizing pH and temperature interference. Integrated with pH and temperature electrochemical sensors, the patch demonstrated reliable on-body performance across multiple body sites, showing strong agreement with ion chromatography. A wireless wearable microfluidic electrochemical sensor for continuous sweat lactate monitoring is presented in^[30]. The sensing platform combines hydrogel with a paper microfluidic channel to facilitate sweat transport and management, demonstrating continuous lactate monitoring over a range of physiological activities while maintaining an ultra-low power consumption profile. The study in^[31] presented a wearable microfluidic-based electrochemical sensor integrated with conducting polymer PEDOT:PSS hydrogel for highly sensitive and accurate detection of UA in sweat with a sensitivity of $0.875 \mu\text{A} \cdot \mu\text{M}^{-1} \cdot \text{cm}^{-2}$ and a LOD of $1.2 \mu\text{M}$. A wearable non-enzymatic flexible microfluidic electrochemical sensor, with an optimized structure by immobilization of Pt/MXene with a conductive hydrogel, was presented in^[32], for continuous measurement of glucose in sweat with potential correlation of glucose in blood. The work in^[33] presented an ultra-high sensitivity, battery-free, and fully integrated wearable microfluidic electrochemical sensing patch for the monitoring of K^+ ions concentration

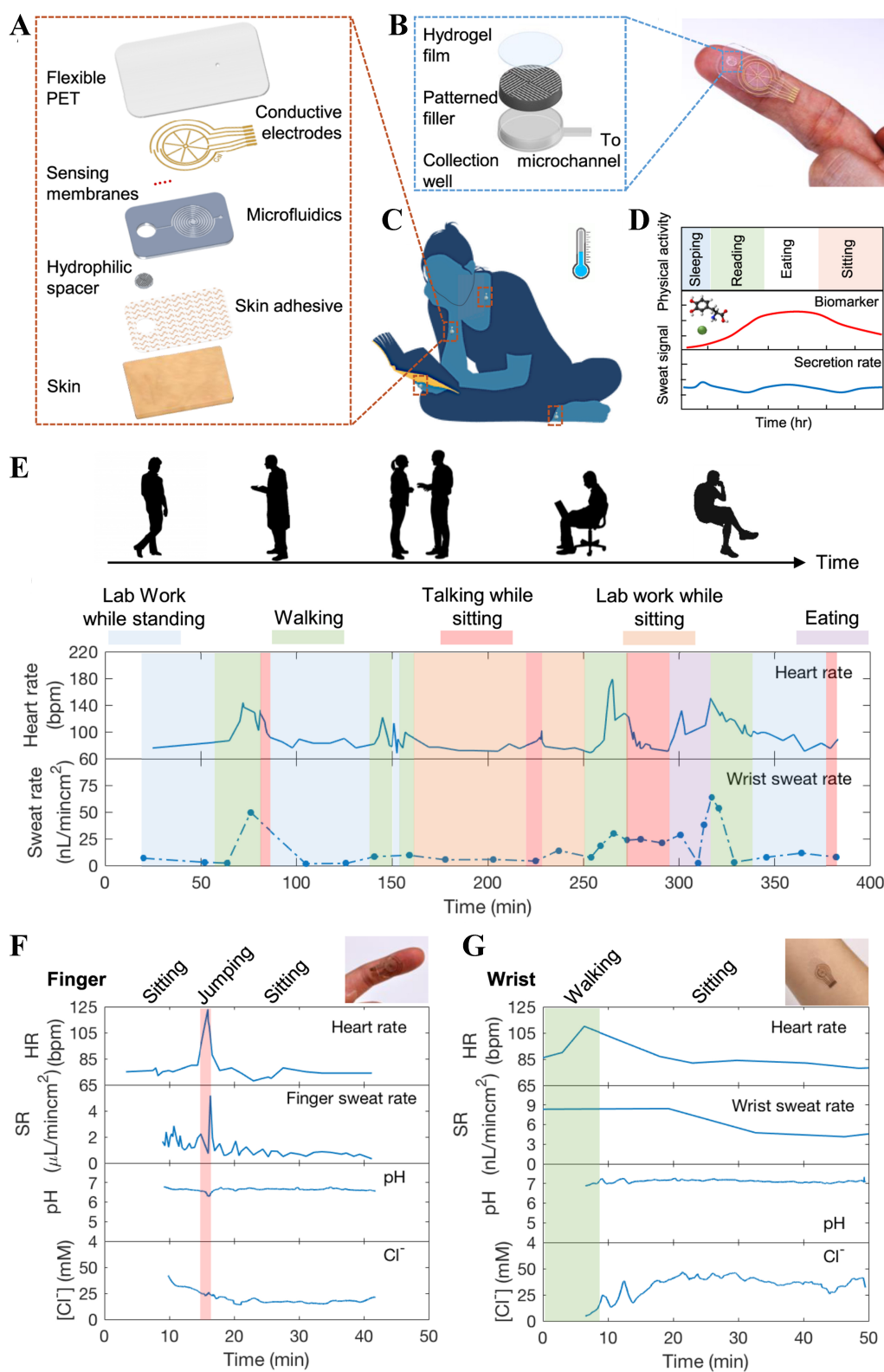


Figure 2. Design and real-time performance monitoring of a wearable microfluidic sweat patch during routine and exercise-related activities. (A) The multilayer patch design comprises a flexible PET substrate with conductive electrodes, sensing membranes, microfluidic channels, hydrophilic filler, and a skin adhesive layer for efficient sweat collection and sensing; (B) The hydrophilic filler structure consisting of a patterned SU-8 mold, PVA film, and hydrogel, facilitating passive sweat uptake into the microchannel by

lowering secretion pressure; (C) Optical image of the patch applied to a user's fingertip and neck; (D) Continuous monitoring of sweat secretion rate and composition for long term without external stimulation; (E) Schematic of long-term biosensing during varied activities such as walking, talking, reading, and eating, illustrating how sweat and biomarker secretion rates vary over time; (F) Continuous monitoring of sweat rate, heart rate, pH, and chloride ion concentration ([Cl]) from the fingertip sensor during various activities; (G) Continuous monitoring of sweat rate, heart rate, pH, and chloride ion concentration ([Cl]) from the wrist sensor. Reprinted with permission from [27], Copyright 2021 Nyein *et al.* PET: Poly (ethylene terephthalate); PVA: polyvinyl alcohol.

in sweat, achieving a concentration sensitivity of 63 mV/dec with excellent selectivity.

Besides single biomarker detection and monitoring, a significant number of studies provide multiplex detection and monitoring of various sweat biomarkers in soft, wearable microfluidic electrochemical devices. The authors in [34] presented a self-powered epidermal microfluidic electrochemical sensor for *in-situ* detection of glucose and lactate in sweat. Enzymatic biofuel cells provide self-power capability facilitating a R^2 score of 0.98 and 0.96 for lactate and glucose, respectively. A novel 3D printed multiplex, low-cost, mechanically flexible, wearable microfluidic electrochemical sensing patch was presented in [35], for noninvasive and simultaneous *ex-situ* and *in-situ* measurement of multiple electrolyte levels in sweat. The study in [36] presented a single universal fully-integrated wearable microfluidic electrochemical sensor array for noninvasive and simultaneous measurement of UA, Na^+ and H^+ in raw sweat, saliva, or urine under various activities. The study in [37] presented a low-cost, laser-cut “smart bandage” microfluidic platform for simultaneous cortisol and glucose detection in sweat. Integrating inkjet-printed electrochemical sensors and a synthetic skin model for realistic perspiration simulation, the device demonstrated high sensitivity (10 pM for cortisol, 10 μM for glucose) and reliable performance at physiological flow rates, highlighting its promise for scalable, noninvasive, multi-biomarker health monitoring.

A comprehensive summary of literature covering wearable electrochemical soft microfluidic sensing platforms is presented in Table 1. The table presents various wearable electrochemical soft microfluidic platforms by highlighting the target analytes, microfluidic technology fabrication and materials, target application domains, and various performance metrics such as LOD, sensitivity, coefficient of determination (R^2) to evaluate the soft sensing platforms.

Colorimetric sensing

Colorimetric sensing techniques have been explored and used over many years due to development of the miniaturization concept and the widespread adoption and popularity of image capture mechanisms. Due to their ease of use and simple applications, colorimetric sensors can be categorized among the widely used sensing platforms in soft, wearable microfluidic systems.

Nutritional health is essential for maintaining physiological homeostasis and preventing disease, and continuous monitoring of key micronutrients can provide actionable insights into the nutritional status of individuals. A promising approach to achieve this goal is through the use of soft, skin-interfaced microfluidic systems capable of real-time, noninvasive nutrient sensing via eccrine sweat analysis. The study in [85] presented a miniaturized, battery-free, and low-cost platform that integrates passive microfluidics, colorimetric assays, and transdermal nutrient delivery to monitor four essential micronutrients, i.e., vitamin C, calcium, zinc, and iron, simultaneously. As illustrated in Figure 3A-C, sweat is routed through laser-patterned microchannels into micro-reservoirs containing colorimetric reagents that produce visible color changes upon interaction with target analytes. The sensor performance is quantitatively analyzed via concentration prediction, RGB image processing, and ultraviolet (UV)–visible spectroscopy as presented in Figure 3D-I for vitamin C, calcium, zinc, and iron. Integration of a nutrient patch enables passive, sustained transdermal delivery, while on-body tests in human volunteers demonstrate the ability of the soft

Table 1. Summary of recent literature on electrochemical sensing using soft microfluidics

Analytes	Microfluidics	Applications	Performance	Ref.
Phe, chloride, pH	PET paper, laser-engraving, and deposition of Cr/Au on PET film by thermal evaporation	Tracking exercise metabolism	LOD: 4.7 μM , sensitivity: 1.4 $\text{nA}\cdot\mu\text{M}^{-1}$	[38]
Glucose	PDMS microfluidic layer, electrochemical sensors were screen-printed over the gold collectors using Ag/AgCl ink	Diverse healthcare and wellness applications	R^2 : 0.90	[39]
	Microfluidic layer with sweat collection and sensing chamber, and cotton thread-based microfluidic channels, glucose sensor anode designed with NPG and PtNP@NPG cathode, Au electrode, mogul substrate, and a waterproof bottom adhesive layer	Wearable glucose sensor	LOD: 9 μM , sensitivity: 62.33 $\text{mV}\cdot\text{M}^{-1}$	[40]
	Silwet-L77 surfactant and PDMS	Personalized healthcare monitoring	LOD: 0.762 μM , R^2 : 0.989	[41]
	Recyclable microfluidic sensing fabric was prepared from the Janus sensing yarn as three electrodes embroidered on a superhydrophobic heated carbon textile	Stable real-time sweat glucose analysis at rest	Sensitivity: 36.57 $\text{mA}\cdot\text{cm}^{-2}\cdot\text{mM}^{-1}$	[42]
	PDMS with PE glycol grafted channels	Potential clinical applications	LOD: 37 μM , sensitivity: 2.7 $\mu\text{A}\cdot\text{mM}^{-1}$, R^2 : 0.9964	[43]
	Ultra-thin skin adhesive, transparent PET layer, microfluidic layer patterned on a double-sided tape enclosed by PET layers, electrochemical sensor electrode layer patterned on a PET substrate	Personalized health monitoring	LOD: 8.9 μM , sensitivity: 10.3 $\text{nA}\cdot\text{cm}^{-2}\cdot\mu\text{M}^{-1}$	[44]
	PI film with fluid inlets, double-sided tape patterned with reservoir and fluid outlet, flexible substrate with Ag/AgCl electrodes	Pathological diagnosis	LOD: 10 μM , sensitivity: 340.68 $\mu\text{A}\cdot\text{mM}^{-1}\cdot\text{cm}^{-2}$	[45]
	Microfluidic channels using transparent PET films	Seamless health monitoring	Sensitivity: 4.75 $\mu\text{A}\cdot\text{mM}^{-1}\cdot\text{cm}^{-2}$	[46]
pH	μCAD fabricated using characterized cotton cloth as support, U-shaped absorbent pad	Personal health assessment	R^2 : 0.997	[47]
	Five layers: (i) PDMS layer; (ii) sebum-adsorption paper (top) layer; (iii) filter paper microfluidic layer; (iv) sebum-adsorption paper (bottom) layer; (v) adhesive tape	Healthcare and diagnostics, sports	LOD: 1 mM	[48]
	Several layers: PDMS cover, PIA, PET film, Ti/Au electrodes, signal transducer, double-sided tape, PIA, microchannel layer, PIA, PDMS cover	Low-cost alternative fabrication method	Sensitivity: 60.8 $\text{mV}\cdot\text{pH}^{-1}$	[49]
UA, Na^+ , K^+ , H^+ , pH	Flexible PET substrate, PI films for sweat and wound exudate transport	Health and wellness monitoring	LOD: 0.3 μM	[50]
UA	PDMS and curing agents uniformly mixed to form a PDMS prepolymer to design microfluidic channels	Personalized healthcare monitoring	LOD: 0.34 μM	[51]
	Flexible electrodes designed using transparent PET membrane by screen-printing, soft PDMS layer for short-circuit prevention, PVC/DOS membrane as protective layer for reference electrodes	Personalized disease prevention	LOD: 0.48 μM	[52]
	PDMS microfluidic collection unit, Ag nanowires@Prussian Blue composite aerogel for UA monitoring	Healthcare	LOD: 50 nM , sensitivity: 50.6 $\mu\text{A}\cdot\text{mM}^{-1}\cdot\text{cm}^{-2}$	[53]
Copper ions	Four layer device: (i) bioadhesive tape; (ii) PET inkjet printed layer; (iii) bioadhesive tape patterned with microfluidic channel and chamber; (iv) PET inkjet-printed layer & personalized and continuous healthcare monitoring	Personalized and continuous healthcare monitoring	LOD: 396 ppb, sensitivity: 2.3 nA/ppb	[54]
	Flexible PDMS-LIG electrodes obtained by stripping the cured PDMS from the PI film, Ag/AgCl coated on LIG as reference electrode, laser-carved microchannels on PDMS, 6 mm cotton thread in the microchannel	Point-of-care testing and detection of heavy-metal ions, sports	LOD: 0.0368 $\mu\text{g}\cdot\text{L}^{-1}$, sensitivity: 0.414 $\mu\text{A}\cdot(\mu\text{g}\cdot\text{L}^{-1})^{-1}\cdot\text{cm}^{-2}$	[55]
Na^+ , K^+ , pH	Three-layer device, PET substrates, gel holding layer patterned on a PMMA substrate by laser cutting	Wearable healthcare	Sensitivity: 61.1 $\text{mV}\cdot\text{dec}^{-1}$	[56]

	Whatman filter paper grade 4, 0.5 mm-thick PE/PP and 0.6 mm thick PE hydrophilic fiber layers, double-sided medical-grade adhesive	Health monitoring during exercise	LOD: H^+ : 10^{-8} M, Na^+ and K^+ : 10^{-3} M, sensitivity: 60 mV·dec ⁻¹	[57]
Glucose, lactate	Laser-induced graphene electrodes, microfluidic device: PE terephthalate and medical adhesive	Personalized wearable diagnostic tools	LOD: (glucose: 8 μ M, lactate: 220 μ M), sensitivity: (glucose: 26.2×10^{-3} μ A·mM ⁻¹ ·cm ⁻²), (lactate 2.47×10^{-3} μ A·mM ⁻¹ ·cm ⁻²)	[58]
	Cover layer, PDMS and PET microfluidic layer, sensor layer with carbon screen-printed electrodes on transparent PET layer, adhesive layer	Personalized and continuous health monitoring	LOD: (glucose: 7.34 μ M), (lactate: 1.24 mM), sensitivity: (glucose: 24.8 μ A·mM ⁻¹ ·cm ⁻²), (lactate: 1.0 μ A·mM ⁻¹ ·cm ⁻²)	[59]
	Adhesive layer using 3M tape and PET, microfluidic channel layer using 3M tape, reservoir layer with 3M tape and PET, electrode layer using PET	Healthcare, diet, and exercise monitoring	LOD: (glucose: 0.55 μ M), (lactate: 0.652 mM), sensitivity: (glucose: 0.002 μ A· μ M ⁻¹), (lactate: 0.0808 μ A·mM ⁻¹)	[60]
K^+ , Na^+	Ion-selective electrodes on PET coated with PEDOT:PSS film, Whatman#4 filter paper for microfluidic device (five layers)	Wearable healthcare	Sensitivity: (K^+ : 58.68 mV·dec ⁻¹), (Na^+ : 62.12 mV·dec ⁻¹)	[61]
Chloride	Several layers: PET substrate, microchannel layer printed on PET film, copper electrode on a PET substrate, sweat inlet layer, chloride ion electrode layer designed on a PET substrate, adhesive layer	Human health forecast and personalized medicine	LOD: 0.9 mM	[62]
UA, dopamine	Top adhesive layer, PI film for flexible sensor electrode, PDMS microfluidic channel, PDMS flexible substrate layer, bottom adhesive layer	Sweat analysis and health monitoring	LOD: (dopamine: 9.41 μ M), (UA: 0.09 μ M), sensitivity: (dopamine: 0.019 μ A· μ M ⁻¹ ·cm ⁻²), (UA: 0.026 μ A· μ M ⁻¹ ·cm ⁻²)	[63]
Glucose, lactate, Na^+ , K^+	PDMS microfluidic chip	Real-time sweat monitoring in sports	Sensitivity: (glucose: 1.3 nA· μ M ⁻¹), (lactate: 210 nA· μ M ⁻¹)	[64]
NaCl	PDMS	Hydration status assessment during exercise	Sensitivity: 20.75 μ S·mM ^{-1/2} , R^2 : 0.995	[65]
Cl^- , Ca^{2+}	PET storage module, Ag/AgCl electrodes on PET layer for sensing module, PET transport module sandwiched between acrylic adhesive layers, simulation module with Ag/AgCl electrodes on PET followed by acrylic adhesive and PMMA gel holder, skin adhesive	Personalized healthcare monitoring	Sensitivity: (Cl^- : 52.3 mV·dec ⁻¹), (Ca^{2+} : 32.9 mV·dec ⁻¹)	[66]
Total ionic change	Electrode layer printed on PI film, Janus textile-embedded hollowed-out microfluidic patch	Personalized physical fitness and health monitoring	Sensitivity: 163.8 mM·L ⁻¹ , R^2 : 0.999	[67]
Lactate	Lactate sensor, double-sided tape, PDMS layers, double-sided tape	Sports and medicine	Sensitivity: 14.5 μ A·mM·cm ⁻²	[68]
Levodopa, UA	PDMS and glass	Personalized healthcare, sports	LOD: (UA: 0.85 μ M), (levodopa: 0.29 μ M), sensitivity: (UA: 0.53 μ A· μ M ⁻¹ ·cm ⁻²), (levodopa: 0.303 μ A· μ M ⁻¹ ·cm ⁻²), R^2 : (UA: 0.9932), (levodopa: 0.9927)	[69]
Riboflavin	Transparent PDMS	Nutrient tracking	LOD: 1.2 nM, sensitivity: 0.0067 μ A·nM ⁻¹	[70]
Dopamine, tyrosine, and paracetamol	The fabrication of TiO ₂ patterns on the flexible PDMS substrate with the growth of a La _{0.85} Sr _{0.15} MnO ₃ sacrificial layer and sequential TiO ₂ multilayers on the clean LaAlO ₃ substrate by polymer-assisted deposition technique	Exercise evaluation and dietary interventions	Sensitivity: (dopamine: 1.390 μ A· μ M ⁻¹ ·cm ⁻²), (tyrosine: 0.126 μ A· μ M ⁻¹ ·cm ⁻²), (paracetamol: 0.0841 μ A· μ M ⁻¹ ·cm ⁻²)	[71]
Levodopa, vitamin C	Flexible sweat patch consists of four parts: microfluidic channel, absorbent pad, electrochemical sensing electrode, and adhesive layer	Personalized healthcare monitoring	LOD: (levodopa: 0.28 μ M), (vitamin C: 17.9 μ M), sensitivity: (levodopa: 0.0073 μ A· μ M ⁻¹), (vitamin C: 0.0018 μ A· μ M ⁻¹)	[72]
Lactate, Na^+ , K^+	Microfluidic module of microfluidic channels was fabricated on the PET film with double-sided tape (2.50 cm × 2.00 cm × 140 μ m) using a CO ₂ laser cutter, adhesive layer on PET film with double-sided tape	Sports	-	[73]

UA, pH, K ⁺	PDMS microfluidic channel layer, insulation layer, electrode layer prepared by screen-printing on PET film, PVC-based ion selective membrane coated onto working electrode, adhesive layer	Personalized health monitoring	LOD: (UA: 4.13 μ M), R ² : 0.9959	[74]
Glucose, pH, total electrolyte concentration	Top PDMS cover, paper-based detection layer, PI film with gold electrodes, PDMS inlet layer, PET adhesive layer with sweat chamber	Sports, clinical care, smart healthcare	LOD: (glucose: 0.0124 mM), R ² : (glucose: 0.99), (pH: 0.96)	[75]
Na ⁺ , pH	Microfluidic device fabricated by a CO ₂ Laser Cutter VEVOR 40W, using Scottex tissue paper as the substrate	Personalized healthcare	R ² : (pH: 0.98), (Na ⁺ : 0.993)	[76]
Glucose, K ⁺	PDMS top layer, flexible PCB, K ⁺ and glucose sensor layer, PMMA-based microfluidic channel layer	Personalized healthcare	Pearson correlation coefficient: 0.99	[77]
UA, Na ⁺ , K ⁺ , pH	PDMS	Health and disease monitoring	Sensitivity: (UA: 51.7 mV·dec ⁻¹), (K ⁺ : 54.4 mV·dec ⁻¹), (pH: 62 mM·pH ⁻¹)	[78]
Glucose, Na ⁺ , K ⁺	PDMS capping layer, PI substrate with electrodes printed with carbon ink containing Prussian Blue, Ag/AgCl ink, and Ag ink, working electrode based on PEDOT:PSS layer and ion selective membrane, PDMS microfluidic layer, skin adhesive layer PMMA microfluidic chip sealed with PDMS	Exercise health monitoring	Sensitivity: (glucose: 981.3 nA·mM ⁻¹)	[79]
Na ⁺	Skin adhesive layer using silicone gel, sensor layer using PET, microfluidic layer using PET, sealing layer using PET	Fitness tracking, geriatric care, and preventive healthcare Personalized healthcare	LOD: (glucose: 2.84 μ M), R ² : 0.99 Sensitivity: 59.3 mV·dec ⁻¹	[80] [81]
Glucose, UA, lactate	PDMS	Personalized health monitoring	LOD: (glucose: 10.83 μ M), (UA: 3.208 μ M), (lactate: 5.274 μ M), sensitivity: (glucose: 15.33 μ A·mM ⁻¹ ·cm ⁻²), (lactate: 219.1 μ A·mM ⁻¹ ·cm ⁻²)	[82]
UA, lactate, pH	Flexible PET patch featuring patterned superhydrophilic and superhydrophobic regions	Individualized wound monitoring	LOD: (UA: 2.2 μ M)	[83]
Dopamine, serotonin, epinephrine	Adhesive layer, PET spacer, and a patterned PET channel layer	Personalized healthcare, mental health diagnostics, and neurophysiological studies	LOD: (dopamine: 0.18 nM), (serotonin: 0.33 nM), (epinephrine: 0.27 nM)	[84]

Phe: Phenylalanine; PET: poly (ethylene terephthalate); LOD: limit of detection; PDMS: polydimethylsiloxane; R²: coefficient of determination; NPG: nanoporous gold; PE: polyethylene; PI: polyimide; μ CAD: microfluidic cloth analytical device; PIA: PDMS-based intermediate adhesive; UA: uric acid; PVC: polyvinyl chloride; DOS: bis(2-ethylhexyl) sebacate; LIG: laser-induced graphene; PMMA: polymethylmethacrylate; PP: polypropylene; PEDOT:PSS: poly(3,4-ethylenedioxythiophene) doped with poly(styrenesulfonate); PCB: printed circuit board.

microfluidic device in tracking dynamic changes in sweat composition following nutrient administration. The data shows strong correlation with blood levels and standard laboratory assays, validating the accuracy and reliability of the platform. This study in^[86] presented a novel, low-cost, and wearable microfluidic thread/fabric-based analytical device (μ TFAD) designed for real-time, noninvasive monitoring of biomarkers in human sweat. Utilizing common textile materials, the μ TFAD is constructed by embroidering hydrophilic threads into a hydrophobic PDMS-treated cotton fabric, creating a network of microchannels and micro-reservoirs that facilitate sweat transport, storage, and analysis without the need for external power or pumping systems. Detection zones, formed from chromogen-treated thread patterns, enable precise colorimetric sensing of sweat pH, chloride, and glucose concentrations. Each sensing region includes a central detection dot surrounded by six reference dots, enabling direct color comparison and RGB-based analysis for enhanced accuracy. On-

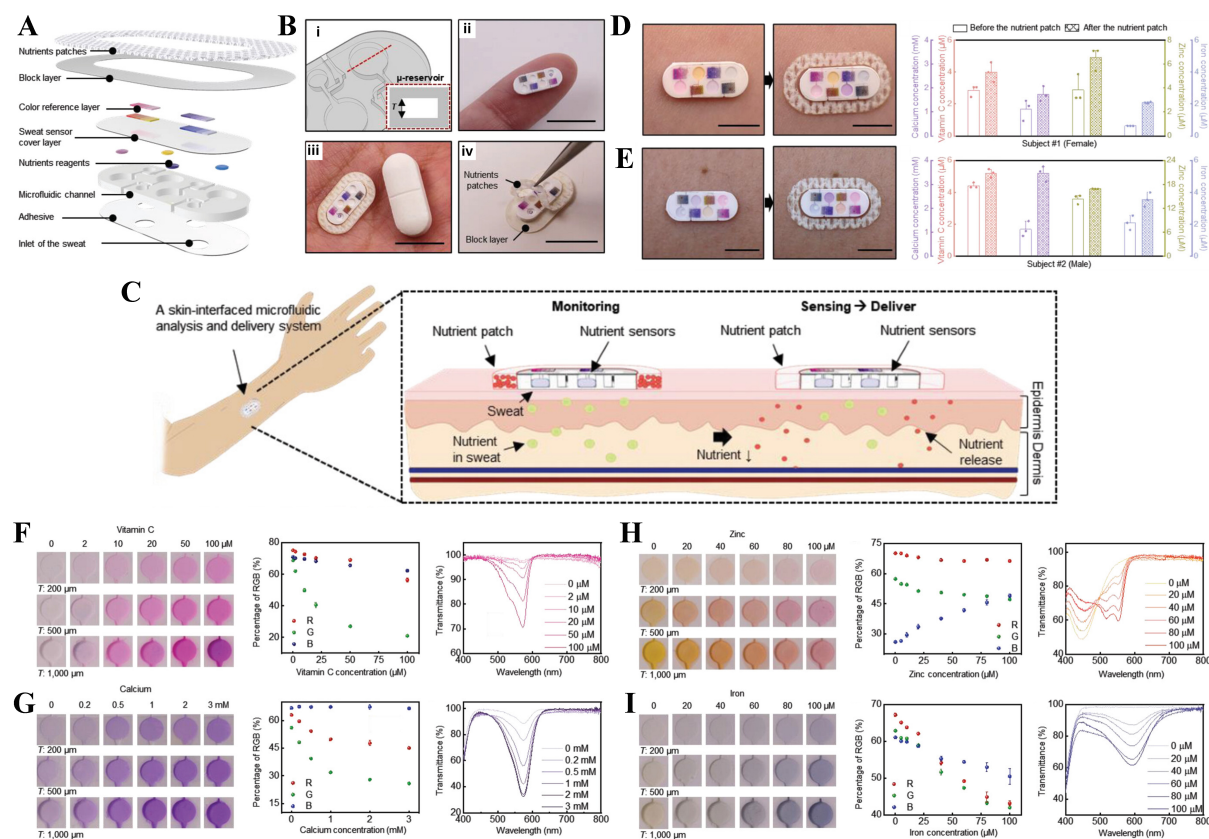


Figure 3. A skin-interfaced miniaturized microfluidic device enabling real-time sweat analysis of four key nutrients (vitamin C, calcium, zinc, and iron) through colorimetric detection and transdermal nutrient delivery. (A-C) Illustration of the device architecture, microreservoir design, and wearable form factor; (D) Images of the device and the concentration of nutrients in sweat before and after sweating with subject#1; (E) Images of the device and the concentration of nutrients in sweat before and after sweating with subject#2; (F-I) Human trials with nutrient monitoring before and after patch application in two subjects and the associated quantitative colorimetric analysis via RGB and UV-Visible spectroscopy validating concentration-dependent responses across varying microreservoir depths, enabling accurate nutrient quantification in sweat. Reprinted with permission from [85], Copyright 2021 Joohee Kim, Yixin Wu, Haiwen Luan, *et al.* *Advanced Science* published by Wiley-VCH GmbH. UV: Ultraviolet.

body validation was conducted with five healthy volunteers, with detection ranges of 5.0–6.0 (pH), 25–80 mM (chloride), and 50–200 μ M (glucose) observed via visual assessment and comparable results (5.47–6.30, 50–77 mM, and 47–66 μ M, respectively) confirmed through smartphone calibration. The LOD reached as low as 10 μ M for glucose, 10 mM for chloride, and pH sensitivity spanned from 4.0 to 9.0.

This study in [87] presented a next-generation wearable microfluidic platform that enables on-demand, longitudinal, and multianalyte sweat analysis, significantly advancing the concept of “lab-on-skin” systems. The device incorporates finger-actuated pumps, valves, and embedded colorimetric sensors into a soft, skin-conformable patch, allowing users to selectively initiate sample analysis at specific times and target condition-specific assays from within a single system as presented in Figure 4A. The design and fabrication methodology supports the seamless integration of multicomponent microfluidic channels, sensing chambers, and pump membranes, all manufactured using cost-effective soft lithography and 3D printing techniques. The system involves customizable sensing chambers containing stacked cellulose membranes, as presented in Figure 4B, for improved fluid distribution, with the optimal configuration (two membrane layers) ensuring uniform analyte interaction. Calibrated colorimetric assays for chloride, calcium, glucose, urea, creatinine, copper, and pH are embedded and validated through RGB image analysis as shown in

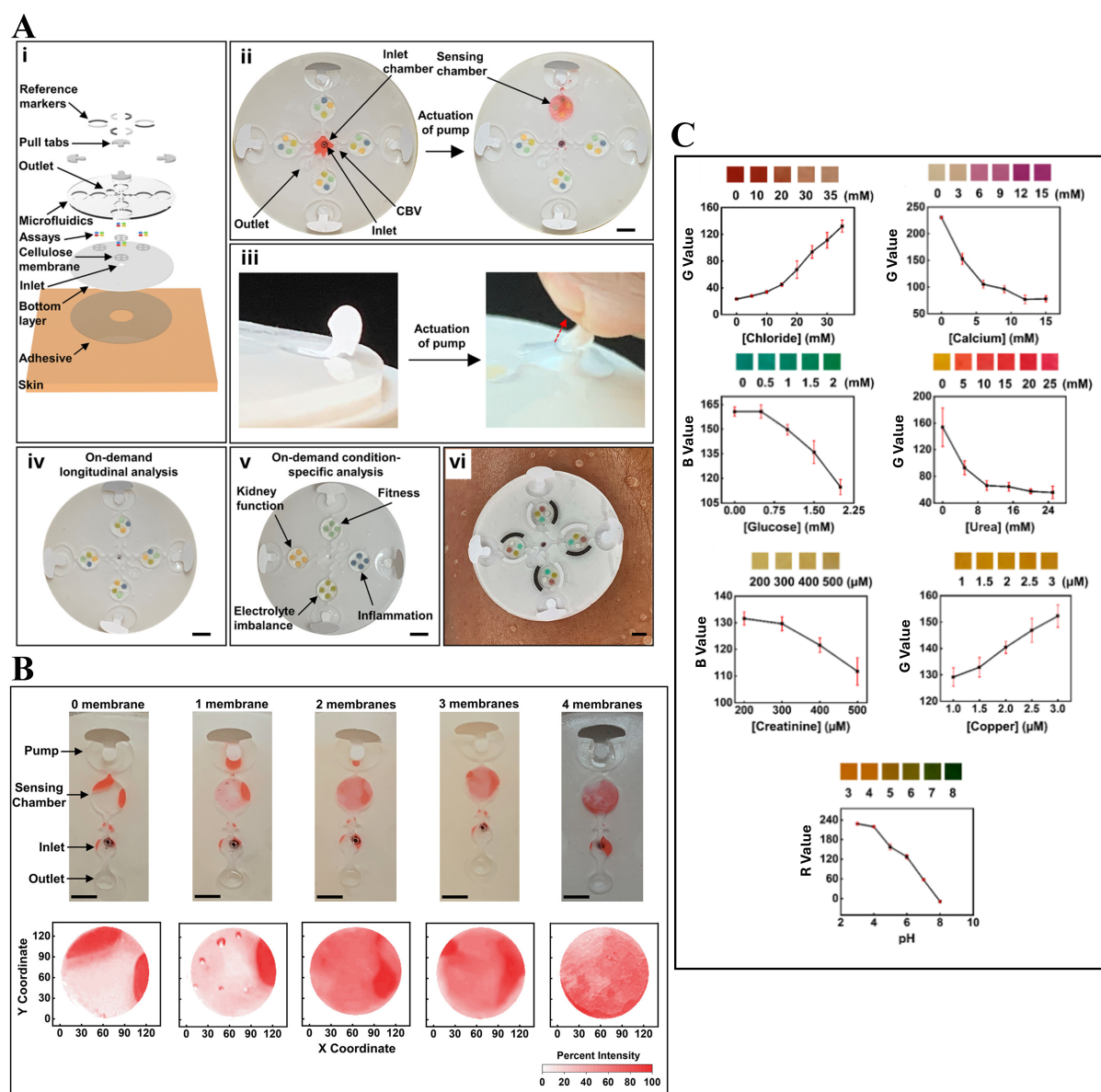


Figure 4. Soft microfluidic wearable patch for on-demand, longitudinal, and multianalyte sweat sensing. (A) Schematic images of the soft microfluidic device, (i) exploded view of the skin-interfaced device, illustrating multilayer components including adhesive backing, microfluidic channels, colorimetric assays, and pull-tab-activated pumps, (ii) Top-down image of the assembled device showing microchambers for targeted fluid delivery, (iii) pump actuation mechanism via manual tab pulling enables selective transport of sweat to designated sensing chambers, (iv) on-demand longitudinal analysis, (v) condition-specific configurations target kidney function, electrolyte imbalance, fitness, and inflammation, (vi) device mounted on a human forearm for on-body testing; (B) Study of sample distribution in sensing chambers using stacked cellulose membranes (0-4), revealing improved color uniformity visualized via 2D pixel intensity heatmaps; (C) (i-vii) Calibration curves of colorimetric assays for chloride, calcium, glucose, urea, creatinine, copper, and pH, respectively, showing RGB intensity values corresponding to concentration gradients. Reprinted with permission from^[87]. Copyright © 2022, American Chemical Society.

Figure 4C. On-body trials over two days involving repeated cycling sessions demonstrate reliable real-time analyte detection (chloride, calcium, glucose, pH), highlighting the potential of the soft microfluidic colorimetric patch for dynamic physiological monitoring, personalized diagnostics, and user-driven health management. The study in^[88] presented a novel class of soft, skin-interfaced, biodegradable microfluidic devices capable of capturing, storing, and analyzing sweat in real time during physical activity and thermal

exposure. Unlike conventional single-use microfluidics, this device emphasizes environmental sustainability by utilizing compostable and enzymatically degradable materials such as thermoplastic copolyester (TPC), cellulose, and naturally derived assay chemistries. The patch, as shown in [Figure 5A](#) and [B](#), integrates colorimetric sensors for chloride and pH, as well as channels for measuring sweat rate and total sweat loss. Anthocyanin and silver chloranilate are used as the sensing chemistries for pH and chloride, respectively, with carefully engineered biocompatibility and degradability. Mechanically, the patch is highly conformable, maintaining function under stretching, bending, and twisting, while its microfluidic geometry supports sequential chrono-sampling via capillary bursting valves as presented in [Figure 5C](#). Human trials conducted during treadmill exercise and sauna exposure, as presented in [Figure 5D](#), demonstrate accurate sweat rate monitoring (0.97 $\mu\text{L}/\text{min}$ in exercise; 0.22 $\mu\text{L}/\text{min}$ in sauna) and analyte quantification as shown in [Figure 5E-G](#). [Figure 5H-J](#) presents that the chloride concentrations were higher during sauna exposure (~ 38 mM) compared to exercise (~ 30 mM), with pH remaining stable (~ 5.2) across both conditions. These results correlate well with known physiological trends and highlight the influence of thermal vs. physical stimuli on sweat composition.

A soft, skin-conformal soft microfluidic sweat sticker enabling efficient, leakage-free collection and smartphone-based quantification of sweat chloride for cystic fibrosis diagnosis is presented in^[89]. Clinical validation confirms the accuracy and usability across various age groups, including infants, offering a noninvasive alternative to traditional methods. This study in^[90] presented a novel wearable microfluidic sweat collection chip incorporating Tesla valves, non-mechanical, diode-like flow structures, to ensure unidirectional sweat flow, minimize backflow, and prevent environmental contamination or evaporation. By optimizing valve geometry and integrating a baffle-structured storage chamber, the device achieves stable, sealed sweat collection. Colorimetric assays for glucose and pH demonstrate its potential for reliable wearable diagnostics. This work in^[91] presented a low-cost, flexible, and skin-attachable colorimetric sweat sensor capable of simultaneously detecting glucose, lactate, urea, and pH, along with sweat loss and skin temperature. Using minimal sweat volume (2.5 μL) and simple fabrication, the device enables rapid, multiplexed, and smartphone-readable analysis, offering a promising solution for home-based, *in-vitro* diagnostics. The study in^[92] introduced a novel class of 3D-printed epidermal microfluidic devices, termed “sweatainers”, that leverage additive manufacturing to create complex, high-resolution microfluidic architectures for wearable sweat sensing. The sweatainer supports a multidraw sweat collection mode, enabling time-segmented, on-body or off-body analysis. The platform integrated colorimetric assays within optically transparent channels, optimized via adaptive printing parameters to ensure dimensional fidelity and signal reliability. A soft, wearable microfluidic patch enabling real-time analysis of sweat rate and chloride concentration in recreational athletes is presented in^[93]. The patch incorporates enlarged collection areas and integrated colorimetric assays, optimized for varying sweat rates. A smartphone app with machine-learning-based image processing ensures accurate readings under uncontrolled lighting and orientations. Field validation across 148 subjects confirms strong agreement with standard absorbent patches, supporting its use in non-clinical, real-world environments. A wearable PDMS-based soft, wearable microfluidic chip for real-time, noninvasive detection of glucose and pH in sweat using smartphone-assisted colorimetric analysis is presented in^[94]. Hydrophilic channels modified with Triton X-100 enable rapid sweat transport to paper-based test strips. Glucose is quantified via GOD-catalyzed H_2O_2 production, while pH is assessed using commercial indicators. Field trials with runners demonstrate the effectiveness of the soft microfluidic platform for dynamic, on-body biochemical monitoring. A paper-based wearable microfluidic sensor with a chrono-sampling design using dissolvable polymer valves for sequential colorimetric measurements is presented in^[95]. Demonstrated through pH and urea sensing, it enables real-time tracking of biomarker fluctuations in sweat using only a smartphone. The work in^[96] presented a soft wearable sensor developed using a plug-type paper-based colorimetric sensor developed onto a PDMS microfluidic chamber using 3D printing for colorimetric sensing of glucose, lactic acid, and pH in sweat.

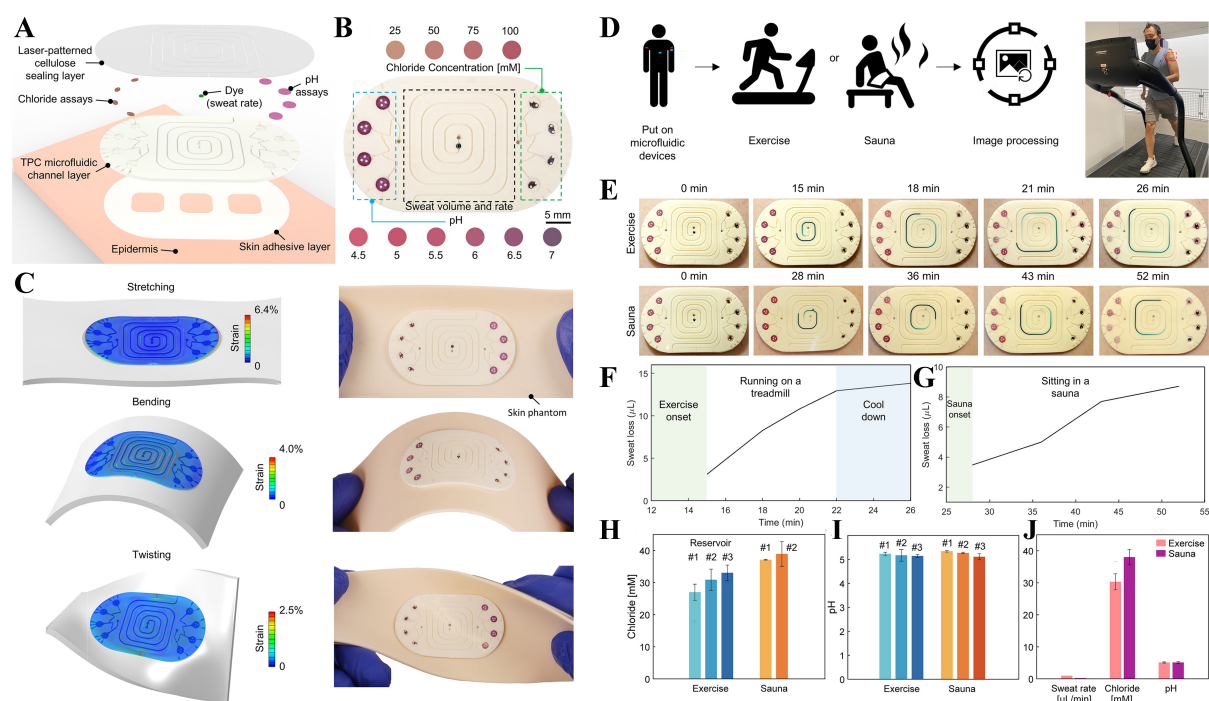


Figure 5. Soft, biodegradable wearable microfluidic devices for sweat analysis under physical and thermal stimuli. (A) Exploded schematic showing the multilayer structure of the biodegradable sweat-sensing patch, comprising a laser-patterned cellulose sealing layer, colorimetric assay reservoirs for chloride and pH, and a TPC microfluidic layer bonded to a skin-adhesive layer; (B) Optical image of the device, highlighting sweat rate/volume channel and biomarker-specific reservoirs with visible colorimetric responses to varying chloride and pH levels; (C) Finite element simulations and corresponding images illustrating mechanical robustness under stretching, bending, and twisting deformations on a silicone skin phantom; (D) Workflow schematic for human trials involving exercise and sauna exposure, followed by digital image analysis; (E) Time-lapse images of the patch during treadmill exercise (first row) and sauna use (second row), respectively, from a human subject, showing progressive filling of microfluidic channels; Quantification of sweat chloride concentration and pH in different reservoirs during (F) exercise and (G) sauna exposure, showing consistent sensor performance; Concentration of (H) chloride and (I) pH value corresponding to each reservoir obtained by colorimetric image processing; (J) Comparative analysis of sweat rate ($\mu\text{L}/\text{min}$), chloride (mM), and pH across exercise and sauna trials. Reprinted from [88], Copyright © 2022 Liu et al. *EcoMat* published by The Hong Kong Polytechnic University and John Wiley & Sons Australia, Ltd. TPC: Thermoplastic copolyester.

A comprehensive literature summary is presented in Table 2. The table presents various wearable colorimetric soft microfluidic platforms by highlighting the target analytes, microfluidic technology fabrication and materials, target application domains, and various performance metrics such as LOD, sensitivity, R^2 to evaluate the soft sensing platforms.

Optical sensing

In microfluidic sensing systems, detection becomes challenging due to low fluid volumes, thereby limiting the number of detectable analytes. As a result, sensitivity and scalability to smaller dimensions are critical factors in selecting suitable detection methods for microfluidic devices. Electrochemical approaches (e.g., conductivity, potential) often struggle in meeting these requirements, especially for sensitive, portable, and wearable applications. Consequently, there is growing interest in integrating optical components into microfluidic platforms. Optical sensing platforms can range from surface-enhanced Raman spectroscopy (SERS) techniques to fluorescence sensing platforms.

The work in [112] developed a soft, flexible, and stretchable wearable plasmonic paper-based microfluidic (paperfluidic) device for real-time, label-free biochemical analysis of human sweat using SERS. As

Table 2. Summary of recent literature on colorimetric sensing in soft microfluidics

Analytes	Microfluidics	Applications	Performance	Ref.
Vitamin C, H ⁺ , Ca ²⁺ , proteins	Top PDMS layer, colorimetric sensing paper chips, PDMS microfluidic channel layer, double-sided medical adhesive as the bottom layer	Health monitoring	R ² : (pH: 0.998), (vitamin C, Ca ²⁺ , proteins: 0.994)	[97]
Glucose, lactate, UA	3D printed microfluidic layers using biocompatible and hydrophobic silicone-based polymeric ink	Health monitoring	LOD: (glucose: 0.038 μM), (lactate: 6.76 μM), (UA: 6.98 μM)	[98]
Chloride	Microfluidic channels and multilayer PDMS device components fabricated via soft photolithography, spin-coating, curing, laser cutting, and plasma bonding	Health monitoring	LOD: 20.12 mM	[99]
VOCs	PDMS	<i>In-situ</i> monitoring of VOCs in fruits	LOD: 5 ppm	[100]
UA	PDMS	Personal health monitoring	LOD: 6.6 μM·L ⁻¹	[101]
Glucose	PSBMA thread-based microfluidic channels and paper-based colorimetric sensor	Personal health monitoring	LOD: 14.7 μM, R ² : 0.98	[102]
	Transparent PI films	Sweat management, physiological information monitoring	LOD: 0.19 mM	[103]
	White plain weave cotton cloth	Low-cost medical diagnostics	R ² : 0.96	[104]
	Outer PDMS contact lens containing microchannels, microchamber, and inlet, paper-based analytical zone embedded in microchambers of the outer lens for colorimetric detection of glucose	Personal health monitoring	LOD: 2 mM	[105]
	Microfluidics layer consisting of a PDMS sheet with microstructured grooves, including a sweat collection inlet, a serpentine channel, a 2D diverter valve, and a 3D gas valve	Long-term glucose monitoring	-	[106]
Glucose, pH	Ultra-thin adhesive bottom layer, PET film encapsulated microfluidic channel layer, filter paper with colorimetric assay, adhesive capping layer	Personal health monitoring	Flow rate: 5 μL·min ⁻¹	[107]
Glucose, chloride	PDMS	Health diagnostics	LOD: (glucose: 1.0 μM), (Cl ⁻ : 100 μM), R ² : (glucose: 0.9979), (Cl ⁻ : 0.9963)	[108]
Lactate	Three-layered PDMS microfluidic chip	Personal health monitoring	LOD: 2.8 mM, R ² : 0.9848	[109]
Glucose, chloride, pH, CoCl ₂	FUNSWTM drinking water test strips (Chloride), Hydrion pH strips (pH), Diastix reagent strips (Glucose), Bartovation cobalt chloride test paper (CoCl ₂)	Ubiquitous personalized health sensing	-	[110]
K ⁺	PDMS cover, hydrogel, Whatman filter paper-based channels, colorimetric paper assay strip for K ⁺ , PDMS casing	Personal health monitoring	LOD: 4.65 mM, R ² : 0.989	[111]

PDMS: Polydimethylsiloxane; R²: coefficient of determination; UA: uric acid; LOD: limit of detection; VOCs: volatile organic compounds; PSBMA: poly(sulfobetaine methacrylate); PI: polyimide; PET: poly (ethylene terephthalate).

illustrated in [Figure 6A-D](#), the device comprises a serpentine microfluidic channel cut from chromatography paper, layered with a plasmonic sensing paper embedded with gold nanorods (AuNRs), a PDMS encapsulation layer, and laser-blocking carbon adhesive, all laminated using a stretchable double-sided adhesive for skin compatibility without irritation. The paperfluidic network facilitates passive sweat transport via capillary action, enabling accurate quantification of sweat loss and rate by monitoring fluid front progression. The plasmonic AuNR paper, prepared through controlled seed-mediated growth and uniform adsorption onto the paper substrate as shown in [Figure 6E](#), exhibited stable optical properties suitable for SERS, with distinct extinction spectra confirming successful integration as presented in [Figure 6F](#). Robust SERS signals were obtained even under probe misalignment as shown in [Figure 6G-I](#), owing to the ratiometric SERS approach and sensor–probe optimization. The device demonstrated reliable *in-situ* detection and quantification of UA in physiologically relevant concentrations, using both benchtop and portable Raman spectrometers as presented in [Figure 6J](#). Human testing confirmed the wearability of

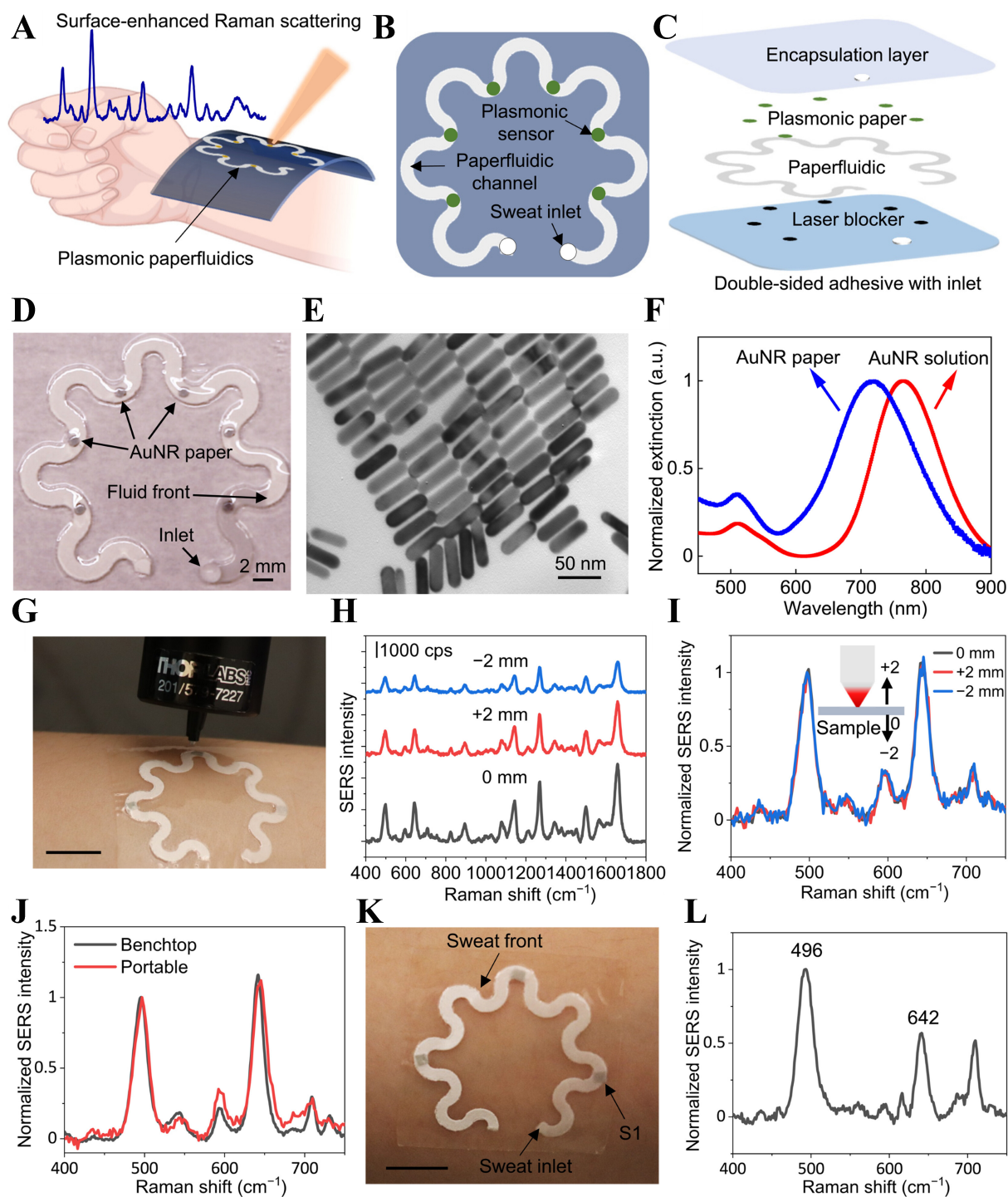


Figure 6. Wearable plasmonic paperfluidic device for sweat analysis using SERS. (A) Conceptual illustration of the device for sweat collection, transport, and *in-situ* analysis; (B) Top view and (C) layered schematic showing the encapsulation layer, paperfluidic channels, plasmonic paper, and laser blocker; (D) Image of the fabricated device with six AuNR-based plasmonic sensors; (E) TEM image of AuNRs; (F) Extinction spectra comparing AuNRs in solution and on paper; (G) A portable Raman spectrometer with a flexible fiber probe for spectra collection; (H) SERS spectra of UA (100 μ M) at different laser distances before and (I) after normalization; (J) SERS spectra comparison between benchtop and portable spectrometers; (K) Image of the device after human wear during exercise; (L) SERS spectrum from sweat collected at sensor. Reprinted with permission from ^[112], Copyright © 2022, The American Association for the Advancement of Science. SERS: Surface-enhanced Raman spectroscopy; AuNR: gold nanorod; TEM: transmission electron microscopy; UA: uric acid.

the wearable paperfluidics sensor during physical activity, as presented in Figure 6K and L, yielding sweat samples suitable for on-body analysis with no adverse effects. Figure 7 illustrates the design and performance of a wearable intelligent sweat platform that enables noninvasive, label-free detection of UA in sweat using SERS^[113]. The device integrates a multilayer structure comprising a paperfluidic layer coated with silver nanowires (AgNWs), PDMS encapsulation and support layers, and medical-grade double-sided adhesive for conformal skin attachment. The AgNWs serve as plasmonic enhancers, enabling sensitive SERS-based detection of UA within the spiral paper channel [Figure 7A and B]. A smartphone interface is used for real-time, visual quantification of sweat volume and pH via image recognition of colorimetric zones [Figure 7C]. As shown in Figure 7D and E, the SERS platform exhibits high sensitivity, detecting UA concentrations as low as 10^{-7} M, with a clear linear correlation between signal intensity at 637 cm^{-1} and UA concentration. Specificity analysis presented in Figure 7F confirms that common sweat constituents such as glucose, urea, and amino acids do not interfere with UA detection. Furthermore, the platform demonstrates reliable SERS performance under varying sweat pH conditions [Figure 7G and H] and across different environments, including PBS, water, and synthetic sweat [Figure 7I]. Collectively, these results highlight the potential of the AgNW-based wearable paperfluidic platform for accurate and intelligent detection of UA in sweat, supporting its application in gout diagnosis and real-time health monitoring. A soft microfluidic nanoplasmonic sensor designed using PDMS microfluidic chip equipped with Ag nanomushroom arrays in SERS chips for sweat sampling and noninvasive detection of lactate, urea, and proteins exhibiting promising correlations between sweat and blood urea concentration is presented in^[114]. Other SERS-based optical sensing studies include core-shell Au nanorods SERS tags integrated onto a textile-based microfluidic device for glucose and lactate monitoring in sweat^[115], Au nanosphere cone arrays-based SERS sensor integrated on a PDMS microfluidics chip for acetaminophen drug monitoring with a LOD of $0.13\text{ }\mu\text{M}$ ^[116], plasmonic paper-based SERS sensor on a PDMS microfluidic device for *in-situ* monitoring of UA and pH value in sweat^[117], PDMS microfluidic chip with erasable liquid metal plasmonic hotspots for precise detection of glucose concentration in sweat^[118], patterned AuNP superlattice film on a PDMS microfluidic chip for pH and lactate detection in sweat^[119], bimetallic self-assembled anti-opal array structure with uniform hotspots SERS sensor integrated into a silk fibron-based microfluidic sensing patch for chemical fingerprinting of sweat creatinine and UA^[120], simultaneous urea and lactate detection using Au-Ag nanoshuttle arrays-based SERS sensor on a PDMS microfluidic platform^[121], dual detection of urea and glucose using Ag nanotripods, for SERS sensing, deposited onto a PDMS microfluidics chip^[122].

Figure 8 illustrates the design and functionality of a microfluidic contact lens sensor developed for real-time, noninvasive detection of glutathione (GSH) in tears, enabling personalized monitoring of OS^[123]. Figure 8A presents the stepwise fabrication process, where UV-pulsed laser ablation forms microchannels on poly((hydroxyethyl)methacrylate-co-ethylene glycol)/polyvinylpyrrolidone [poly(HEMA-co-EG)/PVP] lenses, which are then assembled into a multilayered structure with an encapsulated fluorescent probe that shifts emission from orange [2-cyano-3-(7-(diethylamino)-2-oxo-2H-chromen-3-yl)-N,N-dimethylacrylamide (CCAE)] to light blue [CCAE + GSH conjugate (CCAE-SG)] in response to GSH. The detection mechanism is based on a reversible Michael addition reaction, triggered by GSH and reset by H_2O_2 to simulate OS conditions. Figure 8B presents the smartphone-assisted workflow for practical use, involving tear sample collection, data analysis via a bespoke reader, result display, and device reinitialization for reuse. Figure 8C-K demonstrates the performance of the soft microfluidic fluorescence sensor, including optimization against H_2O_2 levels [Figure 8C and D], temporal dynamics under oxidative conditions [Figure 8E], sensitivity to physiological GSH concentrations [Figure 8F and G], pH and temperature stability [Figure 8H and I], selectivity against common interferents [Figure 8J], and signal reversibility over multiple cycles [Figure 8K], validating its robustness for point-of-care ocular stress monitoring and diagnosis. A fully integrated wearable patch utilizing a QuantumDock-optimized MIP UV-visible spectroscopy sensor onto a laser engraved microfluidic chip enabling continuous, non-invasive monitoring

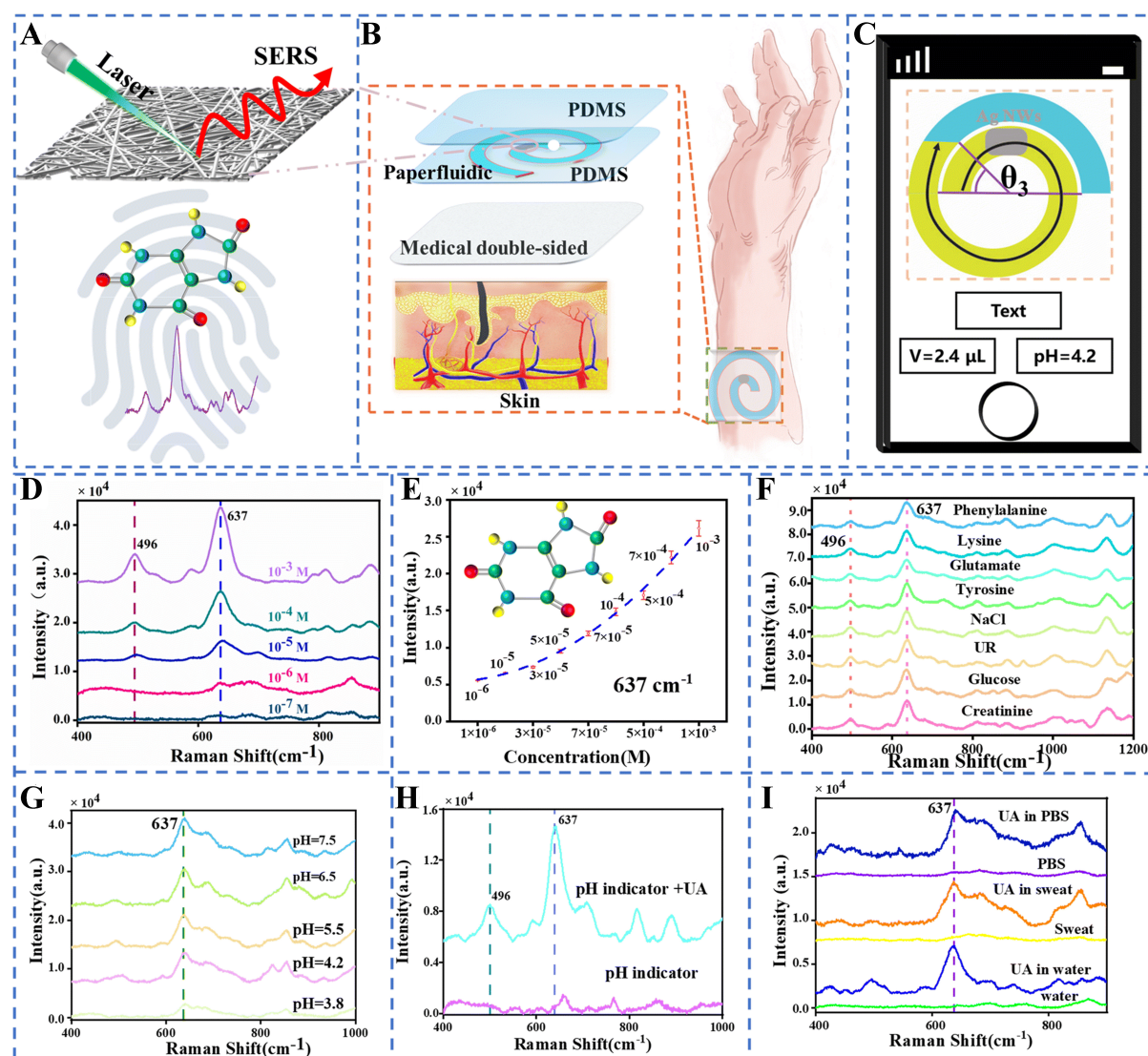


Figure 7. Schematic and performance of a wearable intelligent sweat sensing platform based on SERS. (A) Illustration of the SERS detection mechanism on the plasmonic paperfluidic substrate; (B) Exploded view of the multilayer device structure and skin interface; (C) Smartphone interface displaying the calculated sweat volume and pH value; (D) SERS spectra of UA at concentrations ranging from 10⁻³ to 10⁻⁷ M; (E) Calibration curve showing the polynomial fit of SERS intensity at 637 cm⁻¹ vs. UA concentration; (F) SERS spectra of UA compared with various coexisting analytes, demonstrating spectral selectivity; (G) SERS spectra of UA in sweat across different pH levels; (H) SERS spectra of UA with and without a pH indicator; (I) SERS spectra of UA in different environments, including PBS, sweat, and water. Reprinted with permission from [113], Copyright 2024, Royal Society of Chemistry. SERS: Surface-enhanced Raman spectroscopy; UA: uric acid; PBS: phosphate buffered saline.

of phenylalanine (Phe) in human sweat is presented in [124]. QuantumDock utilizes quantum theory, specifically density functional theory (DFT), to probe molecular interactions between monomers and the target/interference molecules. The device autonomously induces sweat via carbachol iontophoresis and calibrates real-time measurements with built-in Na⁺ and pH sensors. High correlation with gas chromatography-mass spectrometry (GC-MS) results validates its accuracy for personalized health monitoring. A portable, smartphone-integrated four-channel microfluidic device was developed for simultaneous fluorometric detection of I-Tyr, I-Trp, Crt, and NH⁴⁺ in sweat, targeting kidney disease monitoring is presented in [125]. Using carbon polymer dot-based gelatin hydrogels as sensing probes, the device achieves high sensitivity and selectivity with detection limits as low as 1.2–1.5 μM. The work in [126]

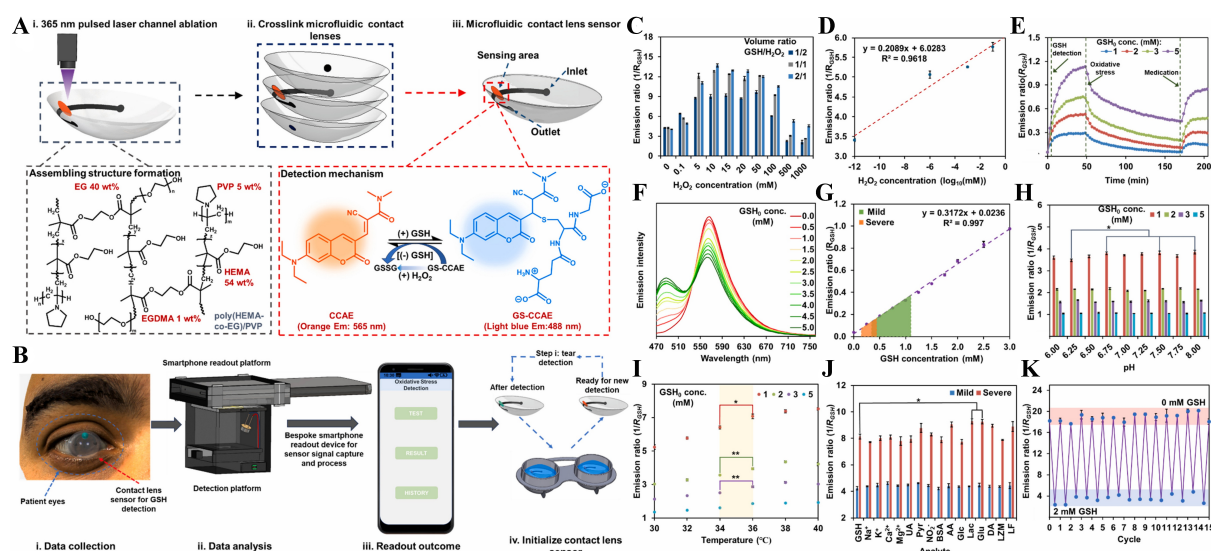


Figure 8. Schematic design and performance validation of a microfluidic contact lens sensor for point-of-care detection of GSH in tears under OS conditions. (A) Fabrication process: (i) UV laser ablation of poly(HEMA-co-EG)/PVP contact lenses to form fluidic channels, (ii) assembly with two non-ablated lenses, and (iii) formation of a sandwiched microfluidic contact lens sensor with inlet, outlet, and sensing area. The embedded CCAE fluorophore undergoes a Michael addition reaction with GSH, shifting fluorescence from orange (565 nm) to light blue (488 nm), and reversibly recovers upon H_2O_2 exposure, simulating OS; (B) Protocol for GSH monitoring: (i) the patient wears the lens for tear collection and detection, (ii) a bespoke smartphone-based readout device captures and processes sensor signals, (iii) data is displayed through a user-friendly app, and (iv) the lens is regenerated in buffer for reuse; (C-K) Evaluation of sensor performance: (C) Optimization of emission ratio (I_{565}/I_{488}) based on GSH: H_2O_2 volume ratio and H_2O_2 concentration, (D) calibration of emission response over a wide range of H_2O_2 concentrations, (E) simulation of dynamic OS and medication effects, (F) emission spectra with increasing GSH concentrations, (G) calibration curves for mild and severe oxidative conditions, (H) stability across physiological tear pH (6.0-8.0), (I) temperature-dependent sensor behavior, (J) selectivity against common tear analytes including UA, ions, glucose, and proteins under mild and severe OS conditions, and (K) demonstration of the reversible sensing ability across 15 detection cycles. Reprinted with permission from [123], Copyright© 2025 Shi *et al.* Published by Elsevier B.V. GSH: Glutathione; OS: oxidative stress; poly(HEMA-co-EG)/PVP: poly((hydroxyethyl)methacrylate-co-ethylene glycol)/polyvinylpyrrolidone; CCAE: 2-cyano-3-(7-(diethylamino)-2-oxo-2H-chromen-3-yl)-N,N-dimethylacrylamide; UA: uric acid.

presented a smartphone-compatible wearable eye patch integrated with a paper-based, multichannel microfluidic fluorescence sensor chip enables noninvasive, multiplexed detection of fluoroquinolone antibiotics in tears. Using dual-mode fluorescent CdTe-lanthanide nanoprobe, the system achieves rapid (< 5 min), ultrasensitive (nanomolar) detection and accurate discrimination of fluoroquinolones using linear discriminant analysis. The study in [127] introduced a smartphone-compatible dual-channel wearable microfluidic platform for real-time, noninvasive monitoring of volatile organic compound (VOC) biomarkers, i.e., acetone and ammonia, in sweat for diabetes tracking. Utilizing carbon polymer dots and carbon dots-based fluorometric hydrogels integrated into cellulose paper, the system achieves highly sensitive detection (0.01 ppm for acetone, 0.08 ppm for ammonia) with excellent selectivity. A fully biodegradable, paper-based wearable nanosensor patch utilizing boric acid-functionalized carbon quantum dots for noninvasive, real-time glucose monitoring in sweat is presented in [128]. Integrated with a cotton-thread microfluidic channel and smartphone-based RGB analysis, the soft microfluidic sensor demonstrated dual fluorescence/colorimetric response with high sensitivity (LOD: ~1.4-2.0 μM) and strong correlation to clinical data. The work presented in [129] introduced a composite nanofiber membrane (CNMF)-based microfluidic chip designed to overcome sweat accumulation and discomfort issues associated with conventional PDMS or paper-based wearable sweat sensors. By integrating a directionally water-transporting CNMF with patterned PDMS, the chip enables efficient, continuous sweat collection and delivery to analysis zones while maintaining skin comfort. The device supports multiplexed fluorescence-based detection of sweat biomarkers and integrates with a portable 3D-printed readout system, offering a

reliable, comfortable, and practical platform for on-body sweat analysis.

Multimodal sensing

Multimodal sensing platforms in soft microfluidics integrate multiple sensing modalities such as electrochemical, colorimetric, optical detection, *etc.*, within flexible, biocompatible substrates. These platforms enable comprehensive, real-time health monitoring by simultaneously capturing diverse physiological signals from biofluids such as sweat, saliva, or tears, enhancing diagnostic accuracy and user comfort in wearable and implantable applications. Figure 9 presents the overall structure and colorimetric sensing performance of the nanofiber-based multimodal microfluidic analysis system developed for wearable sweat monitoring. The exploded schematic view, presented in Figure 9A, illustrates the multilayer configuration of the multimodal soft microfluidic system, composed of a nanofiber-based microfluidic network that integrates both colorimetric sensing and electrochemical sensing modules^[130]. The colorimetric sensor contains functionalized nanofiber films loaded with assay reagents for glucose, lactate, chloride (Cl⁻), pH, and urea detection, while the electrochemical sensor section incorporates enzyme-functionalized electrodes and ion-selective layers interfaced with NFC electronics for wireless data transmission. Figure 9B depicts representative nanofiber assay films, each functionalized for a specific analyte, enabling multiplexed colorimetric detection. Sweat is routed via the system to respective sensing zones, where biomarker-triggered chemical reactions induce color changes. Quantitative analysis is performed by capturing images of the films using a smartphone, and RGB values are extracted via an integrated NFC-based application. The corresponding normalized RGB percentage curves as a function of biomarker concentration are presented in Figure 9C–G. Glucose and lactate detection are based on enzymatic oxidation reactions that produce hydrogen peroxide, which is further catalyzed to induce visible color shifts. Chloride sensing relies on competitive complexation, pH is monitored using a universal indicator, and urea is indirectly measured via urease-catalyzed hydrolysis that alters local pH. These RGB-concentration relationships confirm the accuracy and sensitivity of the colorimetric sensing strategy. The study in^[131] designed an origami-style, paper-based soft microfluidic sweat sensor capable of simultaneously detecting six biomarkers, glucose, lactate, UA, magnesium ions, pH, and cortisol using colorimetric and electrochemical sensors integrated into the soft microfluidic platform. The 3D chip, made from hydrophilic and hydrophobic filter paper, enabled controlled fluid flow and synchronized signal capture. A reusable electrocolorimetric sweat sensing soft microfluidic platform that integrates electrochemical detection with digital colorimetric display via electrophoretic display technology is presented in^[132]. The device enables real-time, low-power, and pH-calibrated lactate monitoring, validated through human trials for detecting the lactate threshold. The electrocolorimetric system combines enzymatic biosensing, microfluidics, and RGB-based pH calibration, offering a promising, multimodal solution for personalized and continuous health monitoring.

This study in^[133] presented a flexible, multimodal, microfluidic-integrated wearable biosensing patch capable of simultaneously monitoring biochemical (glucose, pH, temperature) and electrophysiological (ECG) signals in real-time. The patch uses reduced graphene oxide and Pt NPs for high-sensitivity glucose sensing, a PANI-based pH sensor, and a laser-burned MXene–polyvinylidene fluoride (PVDF) nanofiber-based ECG sensor. The integrated soft microfluidic design improves sweat handling and signal accuracy, while extensive tests confirm the stability, flexibility, and reliability of the system during on-body use. A 3D-printed, skin-compatible soft microfluidic platform with integrated microcuvettes for accurate, *in-situ* sweat analysis is presented in^[133]. The system enables multimodal spectrophotometric and fluorometric detection of biomarkers including copper, chloride, pH, and glucose, using immobilized colorimetric and fluorometric assays. The use of rigid–soft hybrid materials and optimized microcuvette geometry ensures reliable optical readouts, with laboratory-grade sensitivity and minimized interference from ambient light. The study in^[134] presented a cost-effective, cleanroom-free method for fabricating a skin-mountable, liquid metal-based multimodal soft microfluidic sensor using stretchable and sticky PDMS. The platform supports

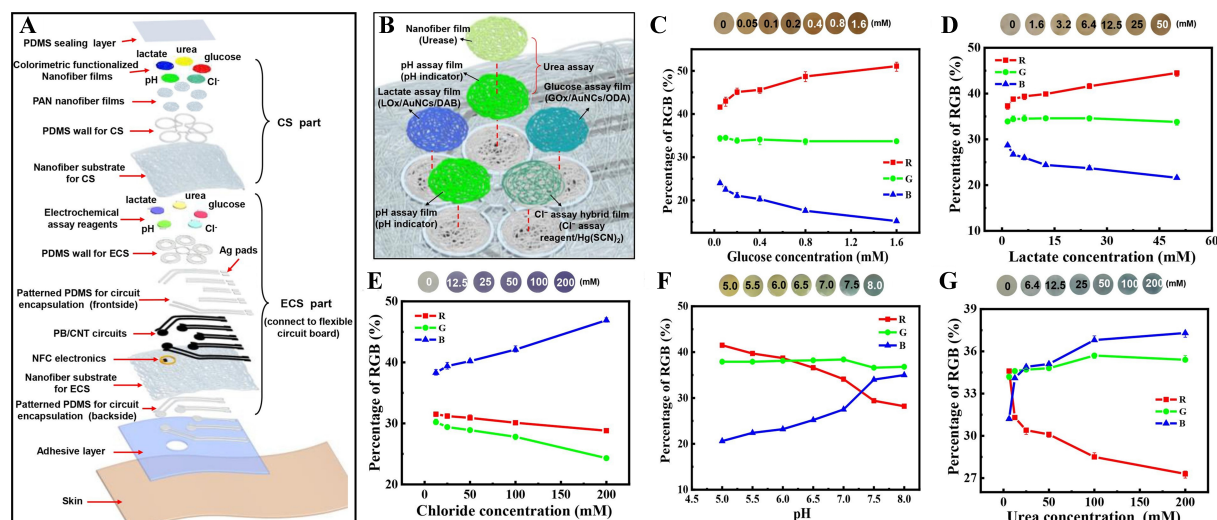


Figure 9. Overall design and colorimetric analysis of the nanofiber-based multimodal analytical system for sweat monitoring. (A) Exploded schematic of the wearable platform showing distinct layers for colorimetric sensing and electrochemical sensing, along with NFC electronics and circuit encapsulation; (B) Functionalized nanofiber films for glucose, lactate, chloride (Cl^-), pH, and urea detection; (C-G) Calibration plots showing normalized RGB percentage responses corresponding to varying concentrations of glucose, lactate, Cl^- , pH, and urea, enabling quantitative sweat biomarker analysis. Reprinted with permission from [130], Copyright © 2022 Elsevier B.V. All rights reserved. NFC: Near field communication.

electromechanical, ECG, and tactile sensing using microfluidic liquid metal channels and gold-laminated electrodes, maintaining robust performance under large deformations. Demonstrated applications include motion detection, electromyogram (EMG)/ECG monitoring, and tactile feedback, highlighting the potential of the multimodal soft microfluidic sensing platform for accessible and versatile healthcare monitoring.

Other sensing mechanisms

A flexible microfluidic triboelectric sensor (FMTS) with 82% optical transmittance is developed in [135] for robust, self-powered human-machine interface applications. The FMTS consists of a PDMS substrate with a 500 μm -deep microchannel, two chambers (liquid and air), interdigitated indium tin oxide (ITO) electrodes, and a 200 μm -thick PDMS triboelectric layer. Upon pressing, liquid flows through the channel, generating quantifiable alternating voltage/current signals via triboelectrification and electrostatic induction. The device exhibits high sensitivity (0.418 kPa^{-1}) over a 2.38–58.12 kPa pressure range and maintains stable performance under bending, twisting, and conformal attachment to skin. Hydrophobic PDMS (contact angle $\approx 134.9^\circ$) ensures efficient contact-separation with deionized water. The FMTS achieves 10° resolution in finger bending angle detection, 99.2% gesture recognition accuracy via machine learning, and up to 98.8% accuracy in identifying eight encoded motion patterns, highlighting its potential for intelligent wearable sensing.

A flexible and biocompatible surface acoustic wave microfluidic pH sensor fabricated on a polyethylene (PE) naphthalate substrate with an aluminum nitride piezoelectric layer is presented in [136]. The device employs interdigitated transducers (IDTs) to generate Lamb waves at $\sim 500 \text{ MHz}$. A microfluidic channel made of SU-8 is aligned between the IDTs and functionalized with ZnO NPs, enabling pH sensitivity via resonance frequency shifts. The sensor exhibits a sensitivity of $\sim 30 \text{ kHz/pH}$ across the pH range 7–2, with clear, reversible frequency shifts due to pH-dependent changes in ZnO NP conductivity. The fabrication process uses bilayer photolithography and microchannel integration without compromising acoustic response. The device shows high reusability, optical transparency, and potential for biosensing applications in wearable platforms.

The work in^[137] presented a novel flexible and wearable pressure sensor designed for integration into cuffless blood pressure monitoring devices. The sensor architecture comprises a soft microfluidic channel encapsulated between two polymer layers: a PET substrate with patterned Au transducers, and a PDMS flexible membrane forming the microfluidic channel filled with electrolyte. External pressure, such as the radial artery pulse waveform, deforms the microchannel, altering the electrical resistance measured by the Au transducers. The fabrication process employs cost-effective, biocompatible materials and standard lithographic techniques, including O₂ plasma treatment and functionalization with silane agents [3-aminopropyl triethoxysilane (APTES) and (3-glycidyloxypropyl)triethoxysilane (GPTES)] to achieve robust bonding between layers. Electrical characterization was conducted using both alternating current and direct current configurations, demonstrating high sensitivity to pressures ranging from 0 to 150 mmHg and stable signal acquisition corresponding to arterial pulse waveforms. The sensor design, with multiple pairs of transducers, enables precise positioning and improved measurement accuracy on the wrist. Another pressure-sensing soft microfluidic system, presented in^[138], aimed at real-time intraocular pressure (IOP) monitoring for glaucoma management. This microfluidic contact lens sensor consists of a bilateral wall structure that significantly improves sensitivity and linearity. Unlike traditional electronic or photonic crystal-based designs, this approach offered enhanced flexibility, low cost, and direct visual readout. Dyed fish oil, chosen for its hydrophilicity, low viscosity, and non-volatility, served as the liquid indicator. The displacement of the fluid interface is automatically tracked using an image processing algorithm. The sensor achieved a high sensitivity of 660 $\mu\text{m}/\text{mmHg}$ with excellent linearity ($R^2 = 0.999$) across the physiological IOP range (10–30 mmHg). The soft microfluidic contact lens demonstrated stable performance over 24 h of static testing and consistent responsiveness to dynamic pressure changes (3 mmHg/s).

DISCUSSION

Despite significant advancements in soft, wearable microfluidic-based biosensors for decentralized and continuous health monitoring, several critical challenges remain before their widespread clinical translation and commercial deployment. Current sensing modalities, including electrochemical, optical, colorimetric, and other systems, each offer unique advantages but still suffer from limitations that hinder long-term stability, reproducibility, and robustness in real-world environments.

Electrochemical sensing platforms, particularly those relying on affinity-based recognition (e.g., antibody–antigen interactions), often face challenges with irreversible binding and degradation of recognition sites over time. Factors such as biofouling, temperature fluctuations, mechanical strain, and long-term exposure to biofluids can lead to sensor deterioration, microcracks in the functional layers, and significant decay in sensitivity and selectivity^[139]. Moreover, redox mediators used in these systems are prone to degradation, limiting sensor longevity and reliability, especially under dynamic, on-skin conditions^[140]. Optical and colorimetric sensing systems offer the benefits of non-contact measurement and direct visual feedback. These sensing platforms also face limitations, particularly in achieving quantitative accuracy under variable lighting conditions and motion artifacts. Environmental interferences such as pH changes, biofluid composition variability, and inconsistent fluid handling can compromise the precision and reliability of such systems^[141]. Additionally, their limited multiplexing capabilities constrain their utility in comprehensive health assessments.

Given these limitations, multimodal sensing platforms are emerging as a powerful strategy in enhancing data reliability, accuracy, and diagnostic coverage. By integrating multiple sensing mechanisms, such as electrochemical, optical, plasmonic, and colorimetric techniques into a unified soft microfluidic platform, it becomes possible to perform cross-validation of signals, compensate for sensor drift, and broaden the detectable biomarker range^[142]. This is particularly vital for detecting low-abundance analytes such as

hormones, proteins, and peptides in noninvasive biofluids such as sweat, tears, or saliva, where concentrations are typically low and poorly correlated with blood levels. Signal amplification approaches, such as aptamer-antibody hybrid recognition and plasmon-enhanced detection (e.g., SERS), can further improve sensitivity for these challenging targets. Moreover, robust integration of soft microfluidics with biosensing components remains a technical bottleneck^[112]. Achieving compatibility between microfluidic channels, bioreceptors, and sensing platforms, while maintaining device stretchability, flexibility, and biocompatibility, is essential. Furthermore, challenges such as microchannel leakage, clogging, or mechanical deformation must be addressed through advanced material engineering and interface design. Mechanical deformation such as twisting, bending, stretching, *etc.*, along with long-term exposure to biofluids, can lead to sensor deterioration and compromise in the sensitivity of the soft microfluidic sensors. Such mechanical deformation problems have been addressed in literature by the use of fabric or thread-based microfluidic platforms offering excellent stretchability, flexibility, and durability, while relying on simple textile processing methods such as weaving, sewing, *etc.*, offering low-cost and rapid processing^[143,144]. Other highly flexible materials such as, PDMS-based soft microfluidic systems^[145], hydrogel paper-based soft microfluidic sensors^[146], provide strain-insensitive systems that can account for motion-induced strain such as stretching, bending, twisting, *etc.*

Furthermore, recent advances in granular hydrogel-enabled wearable electrochemical biosensing platforms, skin-interfaced colorimetric microfluidic devices, and standalone stretchable sensing systems further enrich the landscape of soft wearable microfluidics and open new opportunities for next-generation personalized healthcare technologies. Granular hydrogels, with their intrinsic porosity, reconfigurability, and ionic conductivity, have recently been leveraged to create soft and biocompatible biosensing interfaces that enable robust electrochemical monitoring while maintaining skin comfort and long-term stability^[147,148]. Similarly, skin-mounted colorimetric microfluidic devices have emerged as low-cost, user-friendly systems for on-demand sweat analysis, offering real-time readouts of hydration status, electrolyte balance, and metabolic biomarkers without the need for bulky external instrumentation^[140,149]. Moreover, the development of standalone stretchable sensing platforms that integrate power sources, wireless data transmission, and self-healing materials demonstrates a significant step toward fully autonomous wearable systems capable of continuous, multimodal physiological monitoring^[150,151]. Collectively, these emerging approaches not only expand the functional capabilities of wearable microfluidics but also provide a roadmap for future opportunities, including personalized diagnostics, noninvasive health monitoring, and seamless integration of biosensors into daily life.

Another future prospect for the next generation of wearable soft microfluidic systems is the incorporation of artificial intelligence (AI) methods. AI methods are increasingly vital for both the design of microfluidic architectures such as predictive modeling of elastofluidic behavior, optimization of flow control and actuation, and signal processing such as denoising, pattern recognition, and health state classification from multimodal sensor outputs^[96,97]. AI-assisted analysis can enhance the interpretability of complex, multi-sensor data and allow for real-time feedback and predictive diagnostics^[135]. Moreover, AI-driven hardware optimization could accelerate the development of adaptive, self-calibrating sensors capable of operating reliably in diverse and dynamic physiological environments.

To advance the design of next-generation soft wearable microfluidic systems, it is essential to establish clear manufacturing–structure–property–performance relationships. The choice of fabrication strategy, such as soft lithography, 3D printing, laser micromachining, or roll-to-roll processing, directly influences the microchannel geometry, surface chemistry, and integration of sensing elements, which in turn dictate the fluid handling capabilities, mechanical flexibility, and biocompatibility of the devices^[152–154]. Material

selection, particularly elastomers such as PDMS, hydrogels, and stretchable polymers, defines not only the structural robustness and skin-conformability but also impacts properties such as permeability, optical transparency, and long-term stability under physiological conditions^[155,156]. These structural and material properties strongly correlate with device performance, including sensitivity, selectivity, response time, and user comfort in practical biomedical sensing applications^[157,158]. Establishing systematic manufacturing–structure–property–performance frameworks will therefore provide valuable design rules for optimizing device reliability, scalability, and personalization. Future developments are expected to leverage this knowledge to integrate multifunctional sensors, improve wearability, and enable continuous monitoring across diverse biofluid sources.

As soft microfluidic platforms evolve, interdisciplinary integration will be critical, combining advances in material science (e.g., paper-based^[107], textile-based^[159], and liquid metal microfluidics^[118]), microfabrication (e.g., xurography^[160], 3D printing^[98]), surface engineering (e.g., superhydrophobic surfaces^[9], liquid diodes^[161]), and electronics (e.g., NFC-based data transmission^[162], energy harvesting^[163]) to achieve robust, scalable, and clinically viable systems. Ultimately, to realize the full translational potential of wearable microfluidics, it is essential to consider product development cycles from the outset, incorporating strategies such as technology readiness assessment, design-for-manufacture, and readiness for scale-up. Rigorous clinical validation, user-centric design, and addressing market adoption barriers, such as patient comfort, data privacy, and regulatory compliance, will be pivotal to achieving successful bench-to-bedside deployment.

CONCLUSION

Soft microfluidic sensing platforms represent a promising frontier in wearable diagnostics, offering unique advantages in flexibility, comfort, and continuous monitoring of various biomarkers. While colorimetric, electrochemical, and optical detection strategies each contribute distinct benefits, they face inherent limitations in stability, specificity, and integration for long-term use. Multimodal platforms that combine various sensing mechanisms are poised to overcome the challenges in current biosensing paradigms and enable comprehensive physiological monitoring. However, challenges remain in device robustness, biofluid interfacing, signal reliability, and clinical translation. The integration of AI is expected to play a critical role in optimizing microfluidic design, enhancing data analytics, and enabling intelligent, self-adaptive systems. Future efforts must focus on scalable manufacturing, multimodal sensing integration, and clinical validation to bridge the gap between laboratory innovation and real-world personalized healthcare applications.

DECLARATIONS

Authors' contributions

Conceptualization, writing - original draft, writing - review and editing, visualization, formal analysis, investigation: Ibrahim, M. S.

Visualization, writing - review and editing: Naman, A.; Lee, M. S.; Park, S.; Lee, D.

Supervision: Kwak, Y.

Supervision, funding acquisition, conceptualization: Kim, M.

Availability of data and materials

Not applicable.

Financial support and sponsorship

This research was supported by the Ministry of Science and ICT (MSIT), Korea, under the Information Technology Research Center (ITRC) support program (IITP-2025-RS-2024-00438288) supervised by the

Institute for Information & Communications Technology Planning & Evaluation (IITP).

Conflicts of interest

All authors declared that there are no conflicts of interest.

Ethical approval and consent to participate

Not applicable.

Consent for publication

Not applicable.

Copyright

© The Author(s) 2025.

REFERENCES

1. Zachariah, M. A.; Oliveira-Costa, J. P.; Carter, B. S.; Stott, S. L.; Nahed, B. V. Blood-based biomarkers for the diagnosis and monitoring of gliomas. *Neuro. Oncol.* **2018**, *20*, 1155-61. DOI PubMed PMC
2. Bandari, N.; Dargahi, J.; Packirisamy, M. Tactile sensors for minimally invasive surgery: a review of the state-of-the-art, applications, and perspectives. *IEEE. Access.* **2020**, *8*, 7682-708. DOI
3. Sonner, Z.; Wilder, E.; Heikenfeld, J.; et al. The microfluidics of the eccrine sweat gland, including biomarker partitioning, transport, and biosensing implications. *Biomicrofluidics* **2015**, *9*, 031301. DOI PubMed PMC
4. Katchman, B. A.; Zhu, M.; Blain Christen, J.; Anderson, K. S. Eccrine sweat as a biofluid for profiling immune biomarkers. *Proteomics. Clin. Appl.* **2018**, *12*, e1800010. DOI PubMed PMC
5. Roustit, M.; Blaise, S.; Cracowski, J. L. Trials and tribulations of skin iontophoresis in therapeutics. *Br. J. Clin. Pharmacol.* **2014**, *77*, 63-71. DOI PubMed PMC
6. Assalve, G.; Lunetti, P.; Di Cagno, A.; et al. Advanced wearable devices for monitoring sweat biochemical markers in athletic performance: a comprehensive review. *Biosensors* **2024**, *14*, 574. DOI PubMed PMC
7. Gao, F.; Liu, C.; Zhang, L.; et al. Wearable and flexible electrochemical sensors for sweat analysis: a review. *Microsyst. Nanoeng.* **2023**, *9*, 1. DOI PubMed PMC
8. Khumngern, S.; Jeerapan, I. Synergistic convergence of materials and enzymes for biosensing and self-sustaining energy devices towards on-body health monitoring. *Commun. Mater.* **2024**, *5*, 557. DOI
9. Kashaninejad, N.; Nguyen, N. T. Microfluidic solutions for biofluids handling in on-skin wearable systems. *Lab. Chip.* **2023**, *23*, 913-37. DOI PubMed
10. Sheffield, Z.; Paul, P.; Krishnakumar, S.; Pan, D. Current strategies and future directions of wearable biosensors for measuring stress biochemical markers for neuropsychiatric applications. *Adv. Sci.* **2025**, *12*, e2411339. DOI PubMed PMC
11. Ferreira, R. G.; Silva, A. P.; Nunes-Pereira, J. Current on-skin flexible sensors, materials, manufacturing approaches, and study trends for health monitoring: a review. *ACS. Sens.* **2024**, *9*, 1104-33. DOI PubMed PMC
12. Li, X.; Wang, Q.; Zheng, L.; Xu, T. Smart Janus textiles for biofluid management in wearable applications. *iScience* **2024**, *27*, 109318. DOI PubMed PMC
13. Parupelli, S. K.; Desai, S. The 3D printing of nanocomposites for wearable biosensors: recent advances, challenges, and prospects. *Bioengineering* **2023**, *11*, 32. DOI PubMed PMC
14. Cardoso, S.; Silverio, V. Chapter 2 - Introduction to microfabrication techniques for microfluidics devices. In *Drug delivery devices and therapeutic systems*. Elsevier; 2021. pp. 19-30. DOI
15. Ye, C.; Wang, M.; Min, J.; et al. A wearable aptamer nanobiosensor for non-invasive female hormone monitoring. *Nat. Nanotechnol.* **2024**, *19*, 330-7. DOI PubMed PMC
16. Nah, J. S.; Barman, S. C.; Zahed, M. A.; et al. A wearable microfluidics-integrated impedimetric immunosensor based on Ti₃C₂T_x MXene incorporated laser-burned graphene for noninvasive sweat cortisol detection. *Sens. Actuators. B. Chem.* **2021**, *329*, 129206. DOI
17. Fiore, L.; Mazzaracchio, V.; Serani, A.; et al. Microfluidic paper-based wearable electrochemical biosensor for reliable cortisol detection in sweat. *Sens. Actuators. B. Chem.* **2023**, *379*, 133258. DOI
18. Demuru, S.; Kim, J.; El Chazli, M.; et al. Antibody-coated wearable organic electrochemical transistors for cortisol detection in human sweat. *ACS. Sens.* **2022**, *7*, 2721-31. DOI PubMed
19. Mei, X.; Yang, J.; Yu, X.; Peng, Z.; Zhang, G.; Li, Y. Wearable molecularly imprinted electrochemical sensor with integrated nanofiber-based microfluidic chip for in situ monitoring of cortisol in sweat. *Sens. Actuators. B. Chem.* **2023**, *381*, 133451. DOI
20. Garg, M.; Guo, H.; Maclam, E.; et al. Molecularly imprinted wearable sensor with paper microfluidics for real-time sweat biomarker analysis. *ACS. Appl. Mater. Interfaces.* **2024**, *16*, 46113-22. DOI PubMed PMC

21. Singh, N. K.; Chung, S.; Chang, A. Y.; Wang, J.; Hall, D. A. A non-invasive wearable stress patch for real-time cortisol monitoring using a pseudoknot-assisted aptamer. *Biosens. Bioelectron.* **2023**, *227*, 115097. DOI PubMed
22. Zhao, H.; Zhang, X.; Qin, Y.; et al. An integrated wearable sweat sensing patch for passive continuous analysis of stress biomarkers at rest. *Adv. Funct. Mater.* **2023**, *33*, 2212083. DOI
23. Chakoma, S.; Pei, X.; Qin, H.; et al. A passive, reusable, and resonating wearable sensing system for on-demand, non-invasive, and wireless molecular stress biomarker detection. *Nano. Res.* **2024**, *17*, 7542-56. DOI
24. Ying, Z.; Qiao, L.; Liu, B.; Gao, L.; Zhang, P. Development of a microfluidic wearable electrochemical sensor for the non-invasive monitoring of oxidative stress biomarkers in human sweat. *Biosens. Bioelectron.* **2024**, *261*, 116502. DOI PubMed
25. Luan, Y.; Zhou, Y.; Li, C.; et al. Wearable sensing device integrated with prestored reagents for cortisol detection in sweat. *ACS. Sens.* **2024**, *9*, 2075-82. DOI PubMed
26. Massey, R. S.; Gamero, B.; Prakash, R. System-on-board integrated flexible OEGFET aptasensor for saliva testing of cortisol. In *2022 IEEE International Conference on Flexible and Printable Sensors and Systems (FLEPS)*, Vienna, Austria. July 10-13, 2022. IEEE; 2022. p. 1-4. DOI
27. Nyein, H. Y. Y.; Bariya, M.; Tran, B.; et al. A wearable patch for continuous analysis of thermoregulatory sweat at rest. *Nat. Commun.* **2021**, *12*, 1823. DOI PubMed PMC
28. Vinoth, R.; Nakagawa, T.; Mathiyarasu, J.; Mohan, A. M. V. Fully printed wearable microfluidic devices for high-throughput sweat sampling and multiplexed electrochemical analysis. *ACS. Sens.* **2021**, *6*, 1174-86. DOI PubMed
29. Xuan, X.; Pérez-Ràfols, C.; Chen, C.; Cuartero, M.; Crespo, G. A. Lactate biosensing for reliable on-body sweat analysis. *ACS. Sens.* **2021**, *6*, 2763-71. DOI PubMed PMC
30. Saha, T.; Songkakul, T.; Knisely, C. T.; et al. Wireless wearable electrochemical sensing platform with zero-power osmotic sweat extraction for continuous lactate monitoring. *ACS. Sens.* **2022**, *7*, 2037-48. DOI PubMed
31. Xu, Z.; Song, J.; Liu, B.; et al. A conducting polymer PEDOT:PSS hydrogel based wearable sensor for accurate uric acid detection in human sweat. *Sens. Actuators. B. Chem.* **2021**, *348*, 130674. DOI
32. Li, Q. F.; Chen, X.; Wang, H.; Liu, M.; Peng, H. L. Pt/MXene-based flexible wearable non-enzymatic electrochemical sensor for continuous glucose detection in sweat. *ACS. Appl. Mater. Interfaces.* **2023**, *15*, 13290-8. DOI PubMed
33. Zhang, S.; Zahed, M. A.; Sharifuzzaman, M.; et al. A wearable battery-free wireless and skin-interfaced microfluidics integrated electrochemical sensing patch for on-site biomarkers monitoring in human perspiration. *Biosens. Bioelectron.* **2021**, *175*, 112844. DOI PubMed
34. Huang, X.; Li, J.; Liu, Y.; et al. Epidermal self-powered sweat sensors for glucose and lactate monitoring. *Bio. Des. Manuf.* **2022**, *5*, 201-9. DOI
35. Kim, T.; Yi, Q.; Hoang, E.; Esfandiyarpour, R. A 3D printed wearable bioelectronic patch for multi-sensing and in situ sweat electrolyte monitoring. *Adv. Mater. Technol.* **2021**, *6*, 2001021. DOI
36. Bi, Y.; Sun, M.; Wang, J.; et al. Universal fully integrated wearable sensor arrays for the multiple electrolyte and metabolite monitoring in raw sweat, saliva, or urine. *Anal. Chem.* **2023**, *95*, 6690-9. DOI PubMed
37. Naik, A. R.; Zhou, Y.; Dey, A. A.; et al. Printed microfluidic sweat sensing platform for cortisol and glucose detection. *Lab. Chip.* **2021**, *22*, 156-69. DOI PubMed
38. Zhong, B.; Qin, X.; Xu, H.; et al. Interindividual- and blood-correlated sweat phenylalanine multimodal analytical biochips for tracking exercise metabolism. *Nat. Commun.* **2024**, *15*, 624. DOI PubMed PMC
39. Bolat, G.; De la Paz, E.; Azeredo, N. F.; et al. Wearable soft electrochemical microfluidic device integrated with iontophoresis for sweat biosensing. *Anal. Bioanal. Chem.* **2022**, *414*, 5411-21. DOI PubMed
40. Bae, C. W.; Chinnamani, M. V.; Lee, E. H.; Lee, N. Stretchable non-enzymatic fuel cell-based sensor patch integrated with thread-embedded microfluidics for self-powered wearable glucose monitoring. *Adv. Mater. Interfaces.* **2022**, *9*, 2200492. DOI
41. Zhang, Y.; Yang, Z.; Qiao, C.; et al. Synergistic enhancement of wearable biosensor through Pt single-atom catalyst for sweat analysis. *Biosens. Bioelectron.* **2024**, *258*, 116354. DOI PubMed
42. Zhao, H.; Zhang, L.; Deng, T.; Li, C. Microfluidic sensing textile for continuous monitoring of sweat glucose at rest. *ACS. Appl. Mater. Interfaces.* **2024**, *16*, 19605-14. DOI PubMed
43. Mwaurah, M. M.; Vinoth, R.; Nakagawa, T.; Mathiyarasu, J.; Mohan, A. M. V. A neckband-integrated soft microfluidic biosensor for sweat glucose monitoring. *ACS. Appl. Nano. Mater.* **2024**, *7*, 17017-28. DOI
44. Mirlou, F.; Abbasiasl, T.; Mirzajani, H.; et al. Continuous glycemic monitoring enabled by a Wi-Fi energy-harvesting wearable sweat-sensing patch. *Adv. Mater. Technol.* **2024**, *9*, 2301583. DOI
45. Wang, Z.; Bi, X.; Tang, L.; Sun, H.; Cao, Z.; Jiang, C. In-situ generation of Co-Fe bimetallic electrocatalysts on lignosulfonate-derived graphene by direct laser writing for wearable glucose biosensors. *Sens. Actuators. B. Chem.* **2025**, *432*, 137506. DOI
46. Özkahraman, E. E.; Eroğlu, Z.; Efremov, V.; et al. High-performance black phosphorus/graphitic carbon nitride heterostructure-based wearable sensor for real-time sweat glucose monitoring. *Adv. Mater. Technol.* **2025**, *10*, e00106. DOI
47. Escobedo, P.; Ramos-Lorente, C. E.; Martínez-Olmos, A.; et al. Wireless wearable wristband for continuous sweat pH monitoring. *Sens. Actuators. B. Chem.* **2021**, *327*, 128948. DOI
48. Yang, M.; Sun, N.; Lai, X.; et al. Paper-based sandwich-structured wearable sensor with sebum filtering for continuous detection of sweat pH. *ACS. Sens.* **2023**, *8*, 176-86. DOI PubMed
49. Wei, L.; Fang, G.; Kuang, Z.; et al. 3D-printed low-cost fabrication and facile integration of flexible epidermal microfluidics

- platform. *Sens. Actuators. B. Chem.* **2022**, *353*, 131085. DOI
50. Pei, X.; Sun, M.; Wang, J.; Bai, J.; Bo, X.; Zhou, M. A bifunctional fully integrated wearable tracker for epidermal sweat and wound exudate multiple biomarkers monitoring. *Small* **2022**, *18*, e2205061. DOI PubMed
51. Xiao, J.; Luo, Y.; Su, L.; et al. Hydrophilic metal-organic frameworks integrated uricase for wearable detection of sweat uric acid. *Anal. Chim. Acta.* **2022**, *1208*, 339843. DOI PubMed
52. Chen, F.; Wang, J.; Chen, L.; et al. A wearable electrochemical biosensor utilizing functionalized $\text{Ti}_3\text{C}_2\text{T}_x$ MXene for the real-time monitoring of uric acid metabolite. *Anal. Chem.* **2024**, *96*, 3914-24. DOI PubMed
53. Jiang, D.; Zhu, Y.; Sun, Z.; et al. A silver nanowires@Prussian blue composite aerogel-based wearable sensor for noninvasive and dynamic monitoring of sweat uric acid. *Chem. Eng. J.* **2024**, *486*, 150220. DOI
54. Yang, Q.; Rosati, G.; Abarintos, V.; Aroca, M. A.; Osmá, J. F.; Merkoçi, A. Wearable and fully printed microfluidic nanosensor for sweat rate, conductivity, and copper detection with healthcare applications. *Biosens. Bioelectron.* **2022**, *202*, 114005. DOI PubMed
55. Zhang, Q.; Ma, S.; Zhan, X.; et al. Smartphone-based wearable microfluidic electrochemical sensor for on-site monitoring of copper ions in sweat without external driving. *Talanta* **2024**, *266*, 125015. DOI PubMed
56. Paul, B.; Demuru, S.; Lafaye, C.; Saubade, M.; Briand, D. Printed iontophoretic-integrated wearable microfluidic sweat-sensing patch for on-demand point-of-care sweat analysis. *Adv. Mater. Technol.* **2021**, *6*, 2000910. DOI
57. Rovira, M.; Lafaye, C.; Demuru, S.; et al. Assessing the performance of a robust multiparametric wearable patch integrating silicon-based sensors for real-time continuous monitoring of sweat biomarkers. *Biosens. Bioelectron.* **2024**, *262*, 116560. DOI PubMed
58. Garland, N. T.; Schmieder, J.; Johnson, Z. T.; et al. Wearable flexible perspiration biosensors using laser-induced graphene and polymeric tape microfluidics. *ACS. Appl. Mater. Interfaces.* **2023**, *15*, 38201-13. DOI PubMed
59. Sun, T.; Hui, J.; Zhou, L.; et al. A low-cost and simple-fabricated epidermal sweat patch based on “cut-and-paste” manufacture. *Sens. Actuators. B. Chem.* **2022**, *368*, 132184. DOI
60. Liao, C.; Li, S.; Yang, C.; et al. Wearable epidermal sensor patch with biomimetic microfluidic channels for fast and time-sequence monitoring of sweat glucose and lactate. *Talanta* **2025**, *287*, 127683. DOI PubMed
61. Cao, Q.; Liang, B.; Mao, X.; et al. A smartwatch integrated with a paper-based microfluidic patch for sweat electrolytes monitoring. *Electroanalysis* **2021**, *33*, 643-51. DOI
62. Wei, L.; Lv, Z.; He, Y.; et al. In-situ admittance sensing of sweat rate and chloride level in sweat using wearable skin-interfaced microfluidic patch. *Sens. Actuators. B. Chem.* **2023**, *379*, 133213. DOI
63. Wang, C.; Zhang, Y.; Liu, Y.; et al. A wearable flexible electrochemical biosensor with CuNi-MOF@rGO modification for simultaneous detection of uric acid and dopamine in sweat. *Anal. Chim. Acta.* **2024**, *1299*, 342441. DOI PubMed
64. Niu, J.; Lin, S.; Chen, D.; et al. A fully elastic wearable electrochemical sweat detection system of tree-bionic microfluidic structure for real-time monitoring. *Small* **2024**, *20*, e2306769. DOI PubMed
65. Wang, S.; Liu, M.; Yang, X.; et al. An unconventional vertical fluidic-controlled wearable platform for synchronously detecting sweat rate and electrolyte concentration. *Biosens. Bioelectron.* **2022**, *210*, 114351. DOI PubMed
66. Paul Kunnel, B.; Demuru, S. An epidermal wearable microfluidic patch for simultaneous sampling, storage, and analysis of biofluids with counterion monitoring. *Lab. Chip.* **2022**, *22*, 1793-804. DOI PubMed
67. Liu, M.; Wang, S.; Xiong, Z.; et al. Perspiration permeable, textile embeddable microfluidic sweat sensor. *Biosens. Bioelectron.* **2023**, *237*, 115504. DOI PubMed
68. Shitanda, I.; Ozone, Y.; Morishita, Y.; et al. Air-bubble-insensitive microfluidic lactate biosensor for continuous monitoring of lactate in sweat. *ACS. Sens.* **2023**, *8*, 2368-74. DOI PubMed PMC
69. Peng, H. L.; Zhang, Y.; Liu, H.; Gao, C. Flexible wearable electrochemical sensors based on AuNR/PEDOT:PSS for simultaneous monitoring of levodopa and uric acid in sweat. *ACS. Sens.* **2024**, *9*, 3296-306. DOI PubMed
70. Shi, Z.; Deng, P.; Zhou, L. A.; et al. Wireless and battery-free wearable biosensing of riboflavin in sweat for precision nutrition. *Biosens. Bioelectron.* **2024**, *251*, 116136. DOI PubMed
71. Zhang, T.; Zhu, J.; Xie, M.; et al. Highly sensitive wearable sensor based on (001)-orientated TiO_2 for real-time electrochemical detection of dopamine, tyrosine, and paracetamol. *Small* **2024**, *20*, e2312238. DOI PubMed
72. Ning, Q.; Feng, S.; Sun, Q.; et al. Finger-actuated wireless-charging wearable multifunctional sweat-sensing system for levodopa and vitamin C. *Nano. Res.* **2024**, *17*, 3096-106. DOI
73. Cai, J.; Cao, M.; Bai, J.; et al. Flexible epidermal wearable sensor for Athlete's sweat biomarkers monitoring. *Talanta* **2025**, *282*, 126986. DOI PubMed
74. Mi, Z.; Xia, Y.; Dong, H.; et al. Microfluidic wearable electrochemical sensor based on MOF-derived hexagonal rod-shaped porous carbon for sweat metabolite and electrolyte analysis. *Anal. Chem.* **2024**, *96*, 16676-85. DOI PubMed
75. Wang, W.; Jin, Y.; Huang, Y.; et al. A self-driven multifunctional microfluidic sweat analysis system for efficient sweat collection and real-time monitoring. *Sens. Actuators. B. Chem.* **2024**, *414*, 135920. DOI
76. Fiore, L.; Mazzaracchio, V.; Antinucci, A.; et al. Wearable electrochemical device based on butterfly-like paper-based microfluidics for pH and Na^+ monitoring in sweat. *Mikrochim. Acta.* **2024**, *191*, 580. DOI PubMed PMC
77. Ma, L.; Hou, W.; Ji, Z.; Sun, Z.; Li, M.; Lian, B. Wearable electrochemical sensor for sweat-based potassium ion and glucose detection in exercise health monitoring. *ChemistryOpen* **2024**, *13*, e202300217. DOI PubMed PMC
78. Li, X.; He, X.; Yang, G.; Tian, C.; Xu, T. A wearable sensor patch for joule-heating sweating and comfortable biofluid monitoring. *Sens. Actuators. B. Chem.* **2024**, *419*, 136399. DOI

79. Yin, Y.; Tan, Z.; Zhu, W.; et al. A wearable microfluidic system for efficient sweat collection and real-time detection. *Talanta* **2024**, *274*, 125967. DOI PubMed
80. Xu, W.; Cao, Y.; Shi, H.; et al. Skin-interfaced sweat monitoring patch constructed by flexible microfluidic capillary pump and Cu-MOF sensitized electrochemical sensor. *Talanta* **2025**, *291*, 127895. DOI PubMed
81. Liu, G.; Gong, Z.; Dou, X.; et al. An integrated electrochemical sensor with flexible microfluidic structures for human sweat analysis. *BioChip. J.* **2025**, *19*, 50-61. DOI
82. Chen, M.; Zhang, J.; Ji, G.; et al. Universal flexible wearable biosensors for noninvasive health monitoring. *ACS. Appl. Mater. Interfaces.* **2025**, *17*, 20741-55. DOI PubMed
83. Deng, W.; Sun, M.; Cao, M.; et al. A fully integrated wearable biomimetic microfluidic wound tracker for in situ dynamic monitoring of wound exudate oxygen. *ACS. Nano.* **2025**, *19*, 16163-74. DOI PubMed
84. Fredj, Z.; Marvi, F.; Ullah, F.; Sawan, M. A wearable electrochemical aptasensor based MOF on MOF heterostructure for multi-neurotransmitters monitoring. *Mikrochim. Acta.* **2025**, *192*, 384. DOI PubMed PMC
85. Kim, J.; Wu, Y.; Luan, H.; et al. A skin-interfaced, miniaturized microfluidic analysis and delivery system for colorimetric measurements of nutrients in sweat and supply of vitamins through the skin. *Adv. Sci.* **2022**, *9*, e2103331. DOI PubMed PMC
86. Zhao, Z.; Li, Q.; Chen, L.; et al. A thread/fabric-based band as a flexible and wearable microfluidic device for sweat sensing and monitoring. *Lab. Chip.* **2021**, *21*, 916-32. DOI PubMed
87. Mishra, N.; Garland, N. T.; Hewett, K. A.; Shamsi, M.; Dickey, M. D.; Bandodkar, A. J. A soft wearable microfluidic patch with finger-actuated pumps and valves for on-demand, longitudinal, and multianalyte sweat sensing. *ACS. Sens.* **2022**, *7*, 3169-80. DOI PubMed
88. Liu, S.; Yang, D. S.; Wang, S.; et al. Soft, environmentally degradable microfluidic devices for measurement of sweat rate and total sweat loss and for colorimetric analysis of sweat biomarkers. *EcoMat* **2023**, *5*, e12270. DOI
89. Ray, T. R.; Ivanovic, M.; Curtis, P. M.; et al. Soft, skin-interfaced sweat stickers for cystic fibrosis diagnosis and management. *Sci. Transl. Med.* **2021**, *13*, eabd8109. DOI PubMed PMC
90. Shi, H.; Cao, Y.; Zeng, Y.; et al. Wearable tesla valve-based sweat collection device for sweat colorimetric analysis. *Talanta* **2022**, *240*, 123208. DOI PubMed
91. Yue, X.; Xu, F.; Zhang, L.; et al. Simple, skin-attachable, and multifunctional colorimetric sweat sensor. *ACS. Sens.* **2022**, *7*, 2198-208. DOI PubMed
92. Wu, C. H.; Ma, H. J. H.; Baessler, P.; Balanay, R. K.; Ray, T. R. Skin-interfaced microfluidic systems with spatially engineered 3D fluidics for sweat capture and analysis. *Sci. Adv.* **2023**, *9*, eadg4272. DOI PubMed PMC
93. Baker, L. B.; Seib, M. S.; Barnes, K. A.; et al. Skin-interfaced microfluidic system with machine learning-enabled image processing of sweat biomarkers in remote settings. *Adv. Mater. Technol.* **2022**, *7*, 2200249. DOI
94. Liu, D.; Liu, Z.; Feng, S.; et al. Wearable microfluidic sweat chip for detection of sweat glucose and ph in long-distance running exercise. *Biosensors* **2023**, *13*, 157. DOI PubMed PMC
95. Vaquer, A.; Barón, E.; de la Rica, R. Dissolvable polymer valves for sweat chrono-sampling in wearable paper-based analytical devices. *ACS. Sens.* **2022**, *7*, 488-94. DOI PubMed
96. Shi, H.; Cao, Y.; Xie, Z.; Zhao, Y.; Zhang, C.; Chen, Z. Multi-parameter photoelectric data fitting for microfluidic sweat colorimetric analysis. *Sens. Actuators. B. Chem.* **2022**, *372*, 132644. DOI
97. Wang, Z.; Dong, Y.; Sui, X.; et al. An artificial intelligence-assisted microfluidic colorimetric wearable sensor system for monitoring of key tear biomarkers. *npj. Flex. Electron.* **2024**, *8*, 321. DOI
98. Chen, C.; Fu, Y.; Sparks, S. S.; et al. 3D-printed flexible microfluidic health monitor for *in situ* sweat analysis and biomarker detection. *ACS. Sens.* **2024**, *9*, 3212-23. DOI PubMed PMC
99. Alam, M. S.; Kim, J. K.; Choi, J. Multifunctional wearable system for mapping body temperature and analyzing sweat. *ACS. Sens.* **2023**, *8*, 1980-8. DOI PubMed
100. You, Z.; Zhao, M.; Lu, H.; Chen, H.; Wang, Y. Eye-readable and wearable colorimetric sensor arrays for *in situ* monitoring of volatile organic compounds. *ACS. Appl. Mater. Interfaces.* **2024**, *16*, 19359-68. DOI PubMed
101. Li, F.; Jiang, J.; Shen, N.; et al. Flexible microfluidic colorimetric detection chip integrated with ABTS⁺ and Co@MnO₂ nanzyme catalyzed TMB reaction systems for bio-enzyme free detection of sweat uric acid. *Anal. Chim. Acta.* **2024**, *1299*, 342453. DOI PubMed
102. Wu, L.; Xiong, J.; Xiao, G.; et al. Smart salt-responsive thread for highly sensitive microfluidic glucose detection in sweat. *Lab. Chip.* **2024**, *24*, 776-86. DOI PubMed
103. He, Y.; Wei, L.; Xu, W.; Wu, H.; Liu, A. Laser-cutt ed epidermal microfluidic patch with capillary bursting valves for chronological capture, storage, and colorimetric sensing of sweat. *Biosensors* **2023**, *13*, 372. DOI PubMed PMC
104. Laha, S.; Chakraborty, S. Textile handicraft for equipment-free fabrication of wearable low-cost diagnostic sensors for body-fluid based pathology. *J. Micromech. Microeng.* **2023**, *33*, 034005. DOI
105. Isgor, P. K.; Abbasiasl, T.; Das, R.; Istif, E.; Yener, U. C.; Beker, L. Paper integrated microfluidic contact lens for colorimetric glucose detection. *Sens. Diagn.* **2024**, *3*, 1743-8. DOI PubMed PMC
106. Xu, W.; Lu, L.; He, Y.; Cheng, L.; Liu, A. Long-term detection of glycemic glucose/hypoglycemia by microfluidic sweat monitoring patch. *Biosensors* **2024**, *14*, 294. DOI PubMed PMC
107. Abbasiasl, T.; Mirlou, F.; Istif, E.; Ceylan Koydemir, H.; Beker, L. A wearable paper-integrated microfluidic device for sequential

- analysis of sweat based on capillary action. *Sens. Diagn.* **2022**, *1*, 775-86. DOI
108. Li, T.; Chen, X.; Fu, Y.; Liao, C. Colorimetric sweat analysis using wearable hydrogel patch sensors for detection of chloride and glucose. *Anal. Methods*. **2023**, *15*, 5855-66. DOI PubMed
109. Wu, X.; Jin, D.; Li, M.; Luo, X.; Wang, L. Wearable analytical platform for colorimetric detection of sweat lactate using spherical colloidal photonic crystal hydrogel. *Microchem. J.* **2024**, *200*, 110327. DOI
110. Lee, C.; Yang, D.; Ku, P.; Kao, H. C. SweatSkin: rapidly prototyping sweat-sensing on-skin interface based on microfluidics. *Proc. ACM. Interact. Mob. Wearable. Ubiquitous. Technol.* **2023**, *7*, 1-30. DOI
111. Mukherjee, S.; Pietrosevoli Salazar, S.; Saha, T.; Dickey, M. D.; Velev, O. D. Capillary-osmotic wearable patch based on lateral flow assay for sweat potassium analysis. *Sens. Actuators. B. Chem.* **2024**, *419*, 136383. DOI
112. Mogera, U.; Guo, H.; Namkoong, M.; Rahman, M. S.; Nguyen, T.; Tian, L. Wearable plasmonic paper-based microfluidics for continuous sweat analysis. *Sci. Adv.* **2022**, *8*, eabn1736. DOI PubMed PMC
113. Chen, Z.; Wang, W.; Tian, H.; et al. Wearable intelligent sweat platform for SERS-AI diagnosis of gout. *Lab. Chip.* **2024**, *24*, 1996-2004. DOI PubMed
114. He, X.; Fan, C.; Luo, Y.; Xu, T.; Zhang, X. Flexible microfluidic nanoplasmonic sensors for refreshable and portable recognition of sweat biochemical fingerprint. *npj. Flex. Electron.* **2022**, *6*, 192. DOI
115. Zhao, Z.; Li, Q.; Dong, Y.; Gong, J.; Li, Z.; Zhang, J. Core-shell structured gold nanorods on thread-embroidered fabric-based microfluidic device for *ex situ* detection of glucose and lactate in sweat. *Sens. Actuators. B. Chem.* **2022**, *353*, 131154. DOI
116. Xiao, J.; Wang, J.; Luo, Y.; Xu, T.; Zhang, X. Wearable plasmonic sweat biosensor for acetaminophen drug monitoring. *ACS. Sens.* **2023**, *8*, 1766-73. DOI PubMed
117. Li, Y.; Guo, Y.; Chen, H.; et al. Flexible wearable plasmonic paper-based microfluidics with expandable channel and adjustable flow rate for portable surface-enhanced Raman scattering sweat sensing. *ACS. Photonics.* **2024**, *11*, 613-25. DOI
118. Yuan, Q.; Fang, H.; Wu, X.; et al. Self-adhesive, biocompatible, wearable microfluidics with erasable liquid metal plasmonic hotspots for glucose detection in sweat. *ACS. Appl. Mater. Interfaces.* **2024**, *16*, 66810-8. DOI PubMed
119. Ye, H.; Chen, X.; Huang, X.; et al. Patterned gold nanoparticle superlattice film for wearable sweat sensors. *Nano. Lett.* **2024**, *24*, 11082-9. DOI PubMed
120. Hu, M.; Zhu, K.; Wei, J.; et al. Silk fibroin-based wearable SERS biosensor for simultaneous sweat monitoring of creatinine and uric acid. *Biosens. Bioelectron.* **2024**, *265*, 116662. DOI PubMed
121. Yang, H.; Ji, Y.; Shen, K.; Qian, Y.; Ye, C. Simultaneous detection of urea and lactate in sweat based on a wearable sweat biosensor. *Biomed. Opt. Express.* **2024**, *15*, 14-27. DOI PubMed PMC
122. Xiong, S.; Wang, C.; Zhu, C.; Dong, P.; Wu, X. Dual detection of urea and glucose in sweat using a portable microfluidic SERS sensor with silver nano-tripods and 1D-CNN model analysis. *ACS. Appl. Mater. Interfaces.* **2024**, *16*, 65918-26. DOI PubMed
123. Shi, Y.; Hu, Y.; Zhang, Y.; et al. Microfluidic contact lens for continuous monitoring of ocular oxidative stress. *Biosens. Bioelectron.* **2025**, *280*, 117427. DOI PubMed
124. Mukasa, D.; Wang, M.; Min, J.; et al. A computationally assisted approach for designing wearable biosensors toward non-invasive personalized molecular analysis. *Adv. Mater.* **2023**, *35*, e2212161. DOI PubMed PMC
125. Dashtian, K.; Binabaji, F.; Zare-Dorabei, R. Enhancing on-skin analysis: a microfluidic device and smartphone imaging module for real-time quantitative detection of multianalytes in sweat. *Anal. Chem.* **2023**, *95*, 16315-26. DOI PubMed
126. Yin, S.; Chen, X.; Li, R.; Sun, L.; Yao, C.; Li, Z. Wearable, biocompatible, and dual-emission ocular multisensor patch for continuous profiling of fluoroquinolone antibiotics in tears. *ACS. Nano.* **2024**, *18*, 18522-33. DOI PubMed
127. Binabaji, F.; Dashtian, K.; Zare-Dorabei, R.; Naseri, N.; Noroozifar, M.; Kerman, K. Innovative wearable sweat sensor array for real-time volatile organic compound detection in noninvasive diabetes monitoring. *Anal. Chem.* **2024**, *96*, 13522-32. DOI PubMed
128. Kansay, V.; Dutt Sharma, V.; Srivastava, V.; Batra, N.; Chakrabarti, S.; Bera, M. Wearable, disposable and non-enzymatic fluorescence nanosensor for monitoring sweat glucose through smartphone. *Microchem. J.* **2024**, *201*, 110624. DOI
129. Mei, X.; Zhou, L.; Zhu, L.; Wang, B. Composite nanofiber membrane-based microfluidic fluorescence sensors for sweat analysis. *Anal. Chem.* **2025**, *97*, 492-8. DOI PubMed
130. Mei, X.; Yang, J.; Liu, J.; Li, Y. Wearable, nanofiber-based microfluidic systems with integrated electrochemical and colorimetric sensing arrays for multiplex sweat analysis. *Chem. Eng. J.* **2023**, *454*, 140248. DOI
131. Cheng, Y.; Feng, S.; Ning, Q.; et al. Dual-signal readout paper-based wearable biosensor with a 3D origami structure for multiplexed analyte detection in sweat. *Microsyst. Nanoeng.* **2023**, *9*, 36. DOI PubMed PMC
132. Sung, D.; Han, S.; Kim, S.; et al. Electrophoretic digital colorimetry integrated with electrochemical sweat sensor. *Sci. Adv.* **2025**, *11*, eadu2142. DOI PubMed PMC
133. Zahed, M. A.; Kim, D. K.; Jeong, S. H.; et al. Microfluidic-integrated multimodal wearable hybrid patch for wireless and continuous physiological monitoring. *ACS. Sens.* **2023**, *8*, 2960-74. DOI
134. Kim, B.; Lee, S.; Kim, J. I.; et al. Liquid metal-based multimodal wearable sensor platform enabled by highly accessible microfabrication of PDMS with tuned mechanical properties. *Adv. Mater. Technol.* **2025**, *10*, 2400859. DOI
135. Ge, X.; Gao, Z.; Zhang, L.; et al. Flexible microfluidic triboelectric sensor for gesture recognition and information encoding. *Nano. Energy.* **2023**, *113*, 108541. DOI
136. Piro, L.; Lamanna, L.; Guido, F.; et al. Flexible SAW microfluidic devices as wearable pH sensors based on ZnO nanoparticles. *Nanomaterials* **2021**, *11*, 1479. DOI PubMed PMC

137. Ion, M.; Dinulescu, S.; Firtat, B.; Savin, M.; Ionescu, O. N.; Moldovan, C. Design and fabrication of a new wearable pressure sensor for blood pressure monitoring. *Sensors* **2021**, *21*, 2075. [DOI](#) [PubMed](#) [PMC](#)
138. Yuan, M.; Liu, Z.; Wu, X.; et al. High-sensitive microfluidic contact lens sensor for intraocular pressure visualized monitoring. *Sens. Actuators. A. Phys.* **2023**, *354*, 114250. [DOI](#)
139. Singh, A.; Chowdhury, D. R.; Paul, A. A kinetic study of ferrocenium cation decomposition utilizing an integrated electrochemical methodology composed of cyclic voltammetry and amperometry. *Analyst* **2014**, *139*, 5747-54. [DOI](#) [PubMed](#)
140. Chen, S.; Qiao, Z.; Niu, Y.; et al. Wearable flexible microfluidic sensing technologies. *Nat. Rev. Bioeng.* **2023**, *1*, 950-71. [DOI](#)
141. Li, S.; Ma, Z.; Cao, Z.; Pan, L.; Shi, Y. Advanced wearable microfluidic sensors for healthcare monitoring. *Small* **2020**, *16*, e1903822. [DOI](#) [PubMed](#)
142. Mahato, K.; Saha, T.; Ding, S.; Sandhu, S. S.; Chang, A.; Wang, J. Hybrid multimodal wearable sensors for comprehensive health monitoring. *Nat. Electron.* **2024**, *7*, 735-50. [DOI](#)
143. Liu, X.; Lillehoj, P. B. Embroidered electrochemical sensors for biomolecular detection. *Lab. Chip.* **2016**, *16*, 2093-8. [DOI](#) [PubMed](#)
144. Zhao, Y.; Zhai, Q.; Dong, D.; et al. Highly stretchable and strain-insensitive fiber-based wearable electrochemical biosensor to monitor glucose in the sweat. *Anal. Chem.* **2019**, *91*, 6569-76. [DOI](#) [PubMed](#)
145. Kenry; Yeo, J. C.; Yu, J.; Shang, M.; Loh, K. P.; Lim, C. T. Highly flexible graphene oxide nanosuspension liquid-based microfluidic tactile sensor. *Small* **2016**, *12*, 1593-604. [DOI](#) [PubMed](#)
146. Li, T.; Liang, B.; Ye, Z.; et al. An integrated and conductive hydrogel-paper patch for simultaneous sensing of chemical-electrophysiological signals. *Biosens. Bioelectron.* **2022**, *198*, 113855. [DOI](#) [PubMed](#)
147. Yuk, H.; Lu, B.; Lin, S.; et al. 3D printing of conducting polymers. *Nat. Commun.* **2020**, *11*, 1604. [DOI](#) [PubMed](#) [PMC](#)
148. Lorestani, F.; Zhang, X.; Ataie, Z.; et al. A granular hydrogel-enabled wearable electrochemical biosensing platform for continuous non-invasive sweat lactate detection. *Small* **2025**, *21*, e2502655. [DOI](#) [PubMed](#) [PMC](#)
149. Koh, A.; Kang, D.; Xue, Y.; et al. A soft, wearable microfluidic device for the capture, storage, and colorimetric sensing of sweat. *Sci. Transl. Med.* **2016**, *8*, 366ra165. [DOI](#) [PubMed](#) [PMC](#)
150. Ray, T. R.; Choi, J.; Bhandarkar, A. J.; et al. Bio-integrated wearable systems: a comprehensive review. *Chem. Rev.* **2019**, *119*, 5461-533. [DOI](#) [PubMed](#)
151. Lee, S. H.; Lee, H. J.; Lee, S.; Kim, D.; Kim, H. J.; Sunwoo, S. Intrinsically soft implantable electronics for long-term biosensing applications. *Adv. Sens. Res.* **2025**, *4*, 2500002. [DOI](#)
152. Rogers, J. A.; Ghaffari, R.; Kim, D. H. Stretchable bioelectronics for medical devices and systems. 1st edition. Springer Cham; 2016. [DOI](#)
153. Yuk, H.; Lu, B.; Zhao, X. Hydrogel bioelectronics. *Chem. Soc. Rev.* **2019**, *48*, 1642-67. [DOI](#) [PubMed](#)
154. Hui, Z.; Zhang, L.; Ren, G.; Sun, G.; Yu, H. D.; Huang, W. Green flexible electronics: natural materials, fabrication, and applications. *Adv. Mater.* **2023**, *35*, e2211202. [DOI](#) [PubMed](#)
155. Kim, S.; Lee, B.; Reeder, J. T.; et al. Soft, skin-interfaced microfluidic systems with integrated immunoassays, fluorometric sensors, and impedance measurement capabilities. *Proc. Natl. Acad. Sci. U. S. A.* **2020**, *117*, 27906-15. [DOI](#) [PubMed](#) [PMC](#)
156. Zhao, W.; Wang, Z.; Zhang, J.; et al. Vat photopolymerization 3D printing of advanced soft sensors and actuators: from architecture to function. *Adv. Mater. Technol.* **2021**, *6*, 2001218. [DOI](#)
157. Gao, W.; Emaminejad, S.; Nyein, H. Y. Y.; et al. Fully integrated wearable sensor arrays for multiplexed in situ perspiration analysis. *Nature* **2016**, *529*, 509-14. [DOI](#) [PubMed](#) [PMC](#)
158. Dagdeviren, C.; Shi, Y.; Joe, P.; et al. Conformal piezoelectric systems for clinical and experimental characterization of soft tissue biomechanics. *Nat. Mater.* **2015**, *14*, 728-36. [DOI](#) [PubMed](#)
159. Agustini, D.; Caetano, F. R.; Quero, R. F.; et al. Microfluidic devices based on textile threads for analytical applications: state of the art and prospects. *Anal. Methods* **2021**, *13*, 4830-57. [DOI](#) [PubMed](#)
160. Shahriari, S.; Patel, V.; Selvaganapathy, P. R. Xurography as a tool for fabrication of microfluidic devices. *J. Micromech. Microeng.* **2023**, *33*, 083002. [DOI](#)
161. Yang, C.; Li, W.; Zhao, Y.; Shang, L. Flexible liquid-diode microtubes from multimodal microfluidics. *Proc. Natl. Acad. Sci. U. S. A.* **2024**, *121*, e2402331121. [DOI](#) [PubMed](#) [PMC](#)
162. Lazaro, A.; Villarino, R.; Lazaro, M.; Canellas, N.; Prieto-Simon, B.; Girbau, D. Recent advances in batteryless NFC sensors for chemical sensing and biosensing. *Biosensors* **2023**, *13*, 775. [DOI](#) [PubMed](#) [PMC](#)
163. Guan, S.; Li, J.; Wang, Y.; et al. Multifunctional MOF-derived Au, Co-doped porous carbon electrode for a wearable sweat energy harvesting-storage hybrid system. *Adv. Mater.* **2023**, *35*, e2304465. [DOI](#) [PubMed](#)